Earth and Planetary Science Letters 602 (2023) 117945

Contents lists available at ScienceDirect

Earth and Planetary Science Letters

journal homepage: www.elsevier.com/locate/epsl

Decarbonation of subducting carbonate-bearing sediments and basalts of altered oceanic crust: Insights into recycling of CO_2 through volcanic arcs

Fabio Arzilli [a,b,*], Mike Burton [b], Giuseppe La Spina [c], Colin G. Macpherson [d], Peter E. van Keken [e], Jamie McCann [b]

[a] School of Science and Technology, Geology Division, University of Camerino, Camerino, Italy
[b] Department of Earth and Environmental Sciences, University of Manchester, Manchester, UK
[c] Istituto Nazionale di Geofisica e Vulcanologia-Osservatorio Etneo, Sezione di Catania, Catania, Italy
[d] Department of Earth Sciences, University of Durham, Durham, UK
[e] Earth and Planets Laboratory, Carnegie Institution for Science, Washington, D.C., USA

ARTICLE INFO

Article history:
Received 3 June 2022
Received in revised form 16 November 2022
Accepted 30 November 2022
Available online xxxx
Editor: R. Dasgupta

Keywords:
deep carbon cycle
subduction zone
volcanic arcs
carbon dioxide
metamorphic decarbonation

ABSTRACT

The geological carbon cycle has played a key role in controlling climate throughout Earth's history. For the last ~3 billion years plate tectonics has driven subduction. Subducted slabs have transported CO_2 from the lithosphere, hydrosphere, and atmosphere into the Earth, from where it may be released back to the surface through processes such as arc volcanism or can be stored in the deep interior over geological time. Carbonate-bearing sediments and basalts of altered oceanic crust are the primary media by which carbon is subducted. Therefore, quantifying the depth and amount of CO_2 released from different carbonate-bearing lithologies during subduction is fundamental to understanding whether CO_2 is recycled through arc volcanism or buried in the mantle. The magnitude of CO_2 released from subducting slabs at fore- and sub-arc depths is controlled by processes including ocean crust alteration (i.e., carbonation), metamorphic decarbonation, carbonate dissolution and slab-melting. However, the relative contribution of these processes to overall slab decarbonation is still debated, and will be complex given the variety of sedimentary lithologies and subduction geodynamics. Here, we present a global arc-by-arc lithology-specific analysis of the magnitude of slab CO_2 released purely by metamorphic decarbonation of carbonate-bearing sediment and basalt during subduction of altered oceanic crust, using a thermodynamically rigorous model. We find that metamorphic decarbonation is highly efficient in low carbonate sediments, such as carbonated clay, and in carbonated basalts of altered oceanic crust, causing all of their CO_2 to be removed. Sediments with medium and higher carbonate contents, such as chalk and limestone, are only partially decarbonated, but the combination of metamorphic decarbonation and carbonate dissolution promotes efficient carbon loss. Together they can explain observed magmatic CO_2 emissions in carbonate-rich arcs. Warm slabs, such as Mexico and Cascadia, produce complete metamorphic decarbonation of carbonate minerals beneath fore-arcs. Under more common cold and intermediate thermal regimes metamorphic decarbonation of carbonate minerals occurs at depths between ~80 and 170 km (~2.3 to 5.5 GPa) promoting CO_2 input into the mantle sources of volcanic arcs. Overall, our results demonstrate that sub-arc decarbonation is typically considered an important potential source of slab-derived CO_2, which needs to be considered together with carbonate dissolution to explain observed volcanic CO_2 emissions. In many arcs the modelled CO_2 flux from sediment and basalts of altered oceanic crust into the wedge exceeds the observed CO_2 output suggesting that the mantle wedge and arc lithosphere may sequester some CO_2.

1. Introduction

The geological carbon cycle has played a critical role over Earth's history in controlling climate. The current anthropogenic flux of carbon is two orders of magnitude higher than that of

* Corresponding author at: School of Science and Technology, Geology Division, University of Camerino, Camerino, Italy.
E-mail address: fabio.arzilli@unicam.it (F. Arzilli).

https://doi.org/10.1016/j.epsl.2022.117945

volcanic output (Friedlingstein et al., 2010; Burton et al., 2013; Aiuppa et al., 2019), however, over most of Earth's history the carbon flux to the atmosphere has been dominated by volcanic CO_2 emissions (Wong et al., 2019). Recent studies (e.g., Aiuppa et al., 2019; Werner et al., 2019) show that arc volcanoes are important CO_2 emitters, but the origin of volcanic arc CO_2 is still debated. For these reasons, the deep carbon cycle linked to subduction zones and arc volcanism has been intensely investigated during the past 20 years (e.g., Kerrick and Connolly, 2001a; Dasgupta and Hirschmann, 2010; Johnston et al., 2011; Dasgupta, 2013; Ague and Nicolescu, 2014; Kelemen and Manning, 2015; Aiuppa et al., 2017; Plank and Manning, 2019; Stewart and Ague, 2020; Farsang et al., 2021). Subducting slabs transport carbon from the Earth's surface towards the mantle, and multiple processes can mobilise carbon during subduction, providing a source of volatiles to the fore-arc and mantle wedge, or it may be added to the mantle at greater depths, for example by forming diamond. Subducted inorganic carbon (e.g., $CaCO_3$) and reduced organic carbon reside within subducted sediments (e.g., Clift, 2017), altered oceanic crust (AOC), and serpentinized mantle of the slab. Of these, inorganic carbon is globally the predominant carbon-bearing material in subducting sediments (Clift, 2017; Dutkiewicz et al., 2019; Plank and Manning, 2019) and in the upper basaltic portion of the AOC (Kelemen and Manning, 2015; Gorce et al., 2019; Merdith et al., 2019; Li et al., 2019). The dominant form of carbon in the basalts of the AOC is $CaCO_3$ precipitated in veins as calcite and aragonite. In rare cases carbonated serpentinite can form when mantle peridotite is exposed to seawater (Kelemen et al., 2011), but the overall contribution of carbonated peridotite in most global flux estimates is low (Alt et al., 2013; Plank and Manning, 2019). Therefore, the present understanding is that subducting sediments and AOC basalts comprise the majority of the subducted inorganic carbon (e.g., Kelemen and Manning, 2015; Clift, 2017; Dutkiewicz et al., 2019; Plank and Manning, 2019), that dominates global input fluxes in the mantle wedge. Since subducted carbon can return to the atmosphere as CO_2 through arc volcanism, the fate of sedimentary and AOC carbon during subduction is a key factor in several global geochemical cycles including CO_2 emissions from arc volcanoes, atmospheric CO_2 concentrations in Earth's history, and climate (Fischer et al., 2019; Hilton et al., 2002). However, the balance between the amount of subducted CO_2 returned to the surface through arc magmatism and CO_2 returned to the deep mantle remains a matter of debate (e.g., Kelemen and Manning, 2015; Plank and Manning, 2019).

Several processes control the mobilization of carbon out of subducting slabs towards the mantle wedge at fore and sub-arc depths, including: metamorphic decarbonation (e.g., Gorman et al., 2006; Cook-Kollars et al., 2014), carbonate dissolution (e.g., Frezzotti et al., 2011; Ague and Nicolescu, 2014; Kelemen and Manning, 2015; Farsang et al., 2021), partial melting of the AOC (e.g., Poli, 2015; Martin and Hermann, 2018), and diapirism of sediments intruding into the mantle wedge (Marschall and Schumacher, 2012; Kelemen and Manning, 2015; Chen et al., 2021). Prior molecular modelling studies have suggested that only modest amounts of carbon can be released from subducting slabs through metamorphic decarbonation reactions at depths <70 km (i.e. below fore-arcs; Connolly, 2005; Gorman et al., 2006; Kerrick and Connolly, 2001a,b). These findings concur with experiments indicating that carbonate minerals subducted within AOC basalts can be transported to pressures >5.5 GPa (mantle depths of >170 km) without decarbonation (Poli et al., 2009), in turn suggesting only a minor role for the recycling of CO_2 through arc volcanism. However, this conclusion is difficult to reconcile with voluminous CO_2 released from arc volcanoes (Marty and Tolstikhin, 1998; Sano and Williams, 1996; Wallace, 2005; Burton et al., 2013; Aiuppa et al., 2017, 2019; Wong et al., 2019; Werner et al., 2019) and observations that infer CO_2 contents are commonly elevated in arc magma (Blundy et al., 2010). Recently, several studies suggest that arc magmatism transports substantial volumes of carbon out of mantle wedges (Kelemen and Manning, 2015; Aiuppa et al., 2017; Plank and Manning, 2019). However, the absolute flux of carbon through any arc will depend on the quantity and lithology of subducted sediment, the original amount of CO_2 present in the mantle wedge, and also any potential addition of carbon to the magma during its ascent (Hilton et al., 2002; Macpherson et al., 2010; Troll et al., 2012; Aiuppa et al., 2017; Mason et al., 2017; Aiuppa et al., 2019). The potential involvement of arc crust in the latter case further complicates efforts to determine the location and extent to which subducted carbon is expelled from the slab (Kelemen and Manning, 2015), in turn creating large uncertainties in our understanding of the carbon cycle on Earth.

Thermodynamic modelling of mineral stability improves our understanding of the fate of carbon and other volatiles over a range of conditions within subducting slabs that are difficult to observe directly. Previous models have introduced increasing complexity and drawn on an ever-expanding evidence base regarding carbon behaviour in natural and experimental systems (Kerrick and Connolly, 2001a,b; Connolly, 2005; Gorman et al., 2006; Galvez et al., 2016; Tian et al., 2019a,b). Closed-system models predict negligible metamorphic decarbonation under relatively water-poor conditions (Kerrick and Connolly, 2001a,b). Open-system models do indicate modest metamorphic decarbonation of carbonate minerals when H_2O-rich fluids, derived from elsewhere in the slab, promote release of CO_2 into both fore-arc and mantle wedge while retaining substantial carbonate, that is transported into the mantle beyond sub-arc depths. For example, Gorman et al. (2006) modelled infiltration of subducted sediment by a slab-derived H_2O flux that decreased from the fore-arc to low levels beneath the arc (80–170 km; $\sim$2.3–5.5 GPa). The open-system model, developed by Connolly (2005), used an intermediate thermal regime and showed that dehydration commences at 96 km depth, producing a voluminous source of water-rich fluid from the slab between 136 and 156 km depth. Over this depth range the CO_2 concentration in fluids increased, favouring partial decarbonation at sub-arc depths such that 40–90% of the total carbonate was retained beyond sub-arc depths. A recent thermodynamic model predicts that the solubility of carbon in fluids increases with temperature at depths between $\sim$70 and 100 km (Galvez et al., 2016). The extent to which open-system behaviour couples with the evolving metamorphic assemblage to encourage or inhibit slab decarbonation remains an open and important question, which we aim to address with this work.

Globally, slabs encounter strongly varying thermal conditions during subduction, which should cause the efficiency of carbon remobilization in subduction zones to vary greatly. To date, there has not been a global systematic study of metamorphic decarbonation during subduction that considers the composition of the subducting carbonate-bearing lithologies (Plank and Langmuir, 1998; Plank, 2014; Clift, 2017) within the context of the unique thermal structure and H_2O fluxes released from each slab (Syracuse et al., 2010; van Keken et al., 2011). We have developed a Perple_X (Connolly, 2005) based approach to simulate metamorphic reactions to investigate metamorphic decarbonation efficiency in subducting lithologies (sediments and basalts) along the P-T path of 33 different arc sectors (Fig. 1), that represent the majority of subduction zones on Earth. A range of natural carbonate-bearing lithologies was investigated in order to represent the potential subducting carbonate-bearing sediments and AOC basalts (upper basaltic portion of the oceanic crust) in the modern subduction zones (Fig. 1; Supplementary Table 1). We compare the CO_2 flux produced by metamorphic decarbonation of carbonate-bearing sediments and AOC basalts for each subduction zone with CO_2 fluxes emitted from arc volcanism (Aiuppa et al., 2019; Werner et al., 2019) in

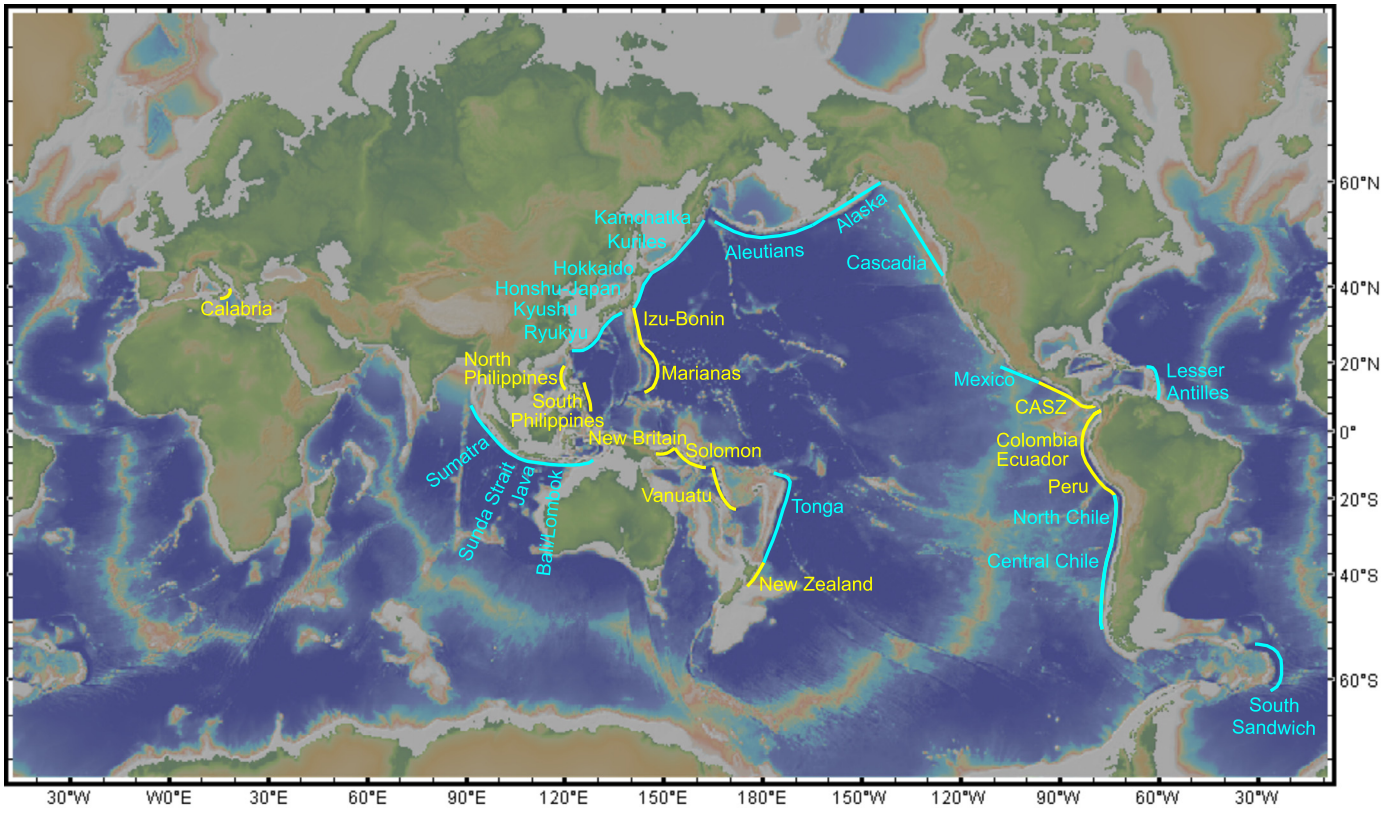

Fig. 1. Global map illustrating the location of the subduction zones considered in this study which have the most active degassing arc volcanoes. The names of the subduction zones have two colours that indicate the presence of carbonate-poor lithologies (cyan) and carbonate-rich lithologies (yellow). CASZ refers to the Central American subduction zones, which includes Guatemala/El Salvador, Nicaragua and Costa Rica. (For interpretation of the colours in the figure(s), the reader is referred to the web version of this article.)

order to quantify the potential contribution of metamorphic decarbonation to the deep carbon cycle on Earth. We also compare the CO_2 flux produced by metamorphic decarbonation with that produced from carbonate dissolution (Farsang et al., 2021).

2. Methods

2.1. Metamorphic decarbonation and fluid flow

Carbonate mineral stability is influenced by the presence of H_2O and CO_2 in subducting rock (Connolly, 2005; Kerrick and Connolly, 2001a). We combine Perple_X (Connolly, 2005) software with a custom-designed algorithm to model incongruent metamorphic decarbonation reactions that lead to the stabilization of calc-silicates, in which only CO_2 is transferred to the fluid and minerals are insoluble, as in a model reaction such as:

$$\text{aragonite} + \text{quartz} = \text{wollastonite} + CO_2$$

The metamorphic decarbonation of subducting carbonate-bearing sediments and carbonated AOC basalts (upper basaltic portion of the oceanic crust) is investigated through an open-system model, in which the volatiles (H_2O and CO_2) are considered as thermodynamic components. We simulate pervasive water infiltration, while allowing removal of CO_2 generated by metamorphic reactions. In this model, we consider the H_2O released from underlying oceanic crust and hydrated mantle lithosphere, in agreement with evidence from previous studies (Ulmer and Trommsdorff, 1995; Schmidt and Poli, 1998). The CO_2 fluxes derived from sediments and AOC basalts through metamorphic decarbonation are calculated separately and then combined. We therefore use two separate models for each margin. Our model simulates a scenario of H_2O infiltration in which grain boundary-fluid interaction dominates simulating pervasive water flow (Fig. 2). The flux of H_2O released at each pressure step of 5 MPa from the serpentinized mantle and the hydrated igneous oceanic crust (~5 km of gabbros and ~1.5 km of basaltic dikes), calculated from van Keken et al. (2011), is transferred to the AOC basalts with a transport rate of 0.25 m yr^{-1} (Wilson et al., 2014). At each pressure step, CO_2 is removed from the system if metamorphic decarbonation occurs and equilibrium is reached (Fig. 2). When stabilization of carbonate minerals is achieved, the quantity of CO_2 in the bulk composition is transferred at the next P-T point (Fig. 2). Metamorphic decarbonation in sediments is calculated with the same approach used for AOC basalts (Fig. 2). The flux of H_2O released at each pressure step of 5 MPa from the serpentinized mantle, hydrated igneous oceanic crust and hydrated sediments, calculated from van Keken et al. (2011), is transferred to the carbonate-bearing sediments considered in this study for each slab with a transport rate of 0.25 m yr^{-1} (Wilson et al., 2014). We use the amount of water predicted by van Keken et al. (2011) for two different purposes. This approach is valid only if a) the decarbonation at lower levels does not affect the H_2O release itself and b) the deep decarbonation does not significantly affect the water composition. Since the main H_2O release in most subduction zones is from the serpentinite and the H_2O does not interact significantly with the carbon-poor gabbros, we satisfy a). The scenario b) was tested and only minor differences were found.

2.2. Subducted sediment and basaltic compositions

The sampling of sedimentary covers and upper oceanic crust offers a direct window into what rocks may eventually subduct and degas (Plank and Langmuir, 1998; Plank, 2014; Clift, 2017).

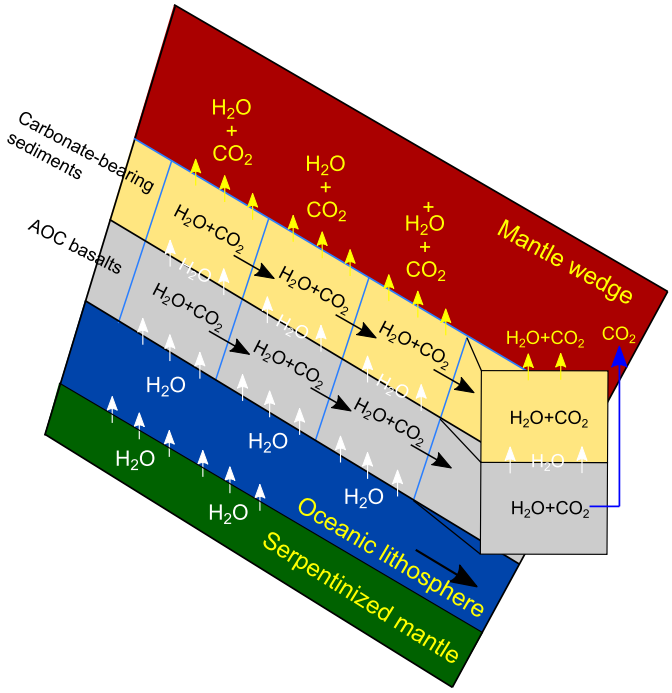

Fig. 2. Schematic depiction of modelling approach. Subduction is modelled by the stepwise variation of pressure and temperature along a path prescribed by a selected thermal model (Syracuse et al., 2010; van Keken et al., 2011). Metamorphic decarbonation is investigated within AOC basalts and carbonate-bearing sediments. Two separate models are run for each margin, therefore, the CO_2 fluxes derived from sediment and AOC basalt through metamorphic decarbonation are calculated separately and summed after. H_2O infiltration between grains is simulated in our model. The flux of H_2O released at each pressure step of 5 MPa from the serpentinized mantle and the oceanic crust (van Keken et al., 2011), is transferred to the AOC basalts with a transport rate of 0.25 m yr^{-1} (Wilson et al., 2014). CO_2 is removed from the system when metamorphic decarbonation occurs at each iteration. After carbonate minerals are stabilized, the CO_2 of the bulk composition is transferred at the next P-T condition. The flux of H_2O released from the AOC basalts every 5 MPa is transferred to the sediments. Metamorphic decarbonation is investigated within the sediments every 5 MPa using the P-T paths of each subduction zone (Syracuse et al., 2010; van Keken et al., 2011).

The amount of inorganic carbon can be heterogeneous and vary widely in composition within subducting sediments (Plank and Langmuir, 1998; Plank, 2014; Clift, 2017; Dutkiewicz et al., 2019). The sedimentary veneer may also have variable thickness along the trench causing heterogeneity in the amount of carbon that can be transported to depth. We modelled the subduction of the most representative carbonate-bearing lithology observed at the trench of each subduction zone investigated (Plank and Langmuir, 1998; Plank, 2014; Clift, 2017) (Supplementary Table 1). The carbonate-poor lithologies are typically represented by siliceous ooze and carbonated clay (< 5 wt.% CO_2 in the bulk composition), whereas carbonate-rich lithologies are represented by calcareous nannofossil ooze, chalk, and limestones with 12–34 wt.% CO_2 in the bulk composition (Plank and Langmuir, 1998; Plank, 2014; Clift, 2017). Terrigenous sediments are excluded in this model, as they can contain little carbonate with more abundant organic carbon. Furthermore, terrigenous sediments are mostly scraped off the slab in the accretionary prism (House et al., 2019).

AOC inorganic carbon is predominant in the upper basaltic portion (300 m of thickness) of the altered oceanic crust (Kelemen and Manning, 2015; Gorce et al., 2019; Merdith et al., 2019; Li et al., 2019). We modelled stable mineral assemblages and metamorphic decarbonation along each subduction geotherm, using a typical carbonated AOC basalt (Staudigel et al., 1989) (Supplementary Table 1).

2.3. Subduction thermal regimes and computational method

In this study we use two-dimensional thermal modelling developed by Syracuse et al. (2010) and van Keken et al. (2011), and specifically their D80 case, in order to investigate the effect of the thermal regime of 33 slabs on metamorphic reactions in subducting lithologies. These arc regions were selected as they have well-constrained quantifications of magmatic gas emissions (Aiuppa et al., 2019; Werner et al., 2019). In the D80 case, the slab couples to the overriding mantle wedge at 80 km which leads to formation of a cold corner and a reduction of convection in the mantle wedge directly above the shallow slab (Abers et al., 2017, 2020). We focused specifically on the P-T paths of the sedimentary and AOC basaltic layers as used by van Keken et al. (2011).

Thermodynamic modelling was computed employing the Gibbs free-energy minimization approach using the software Perple_X (version 6.7.5; Connolly, 2005, 2009) and the thermodynamic database reported from Holland and Powell (2011). The Pitzer & Sterner fluid equation of state (PSEoS) (Pitzer and Sterner, 1994; Holland and Powell, 2003) was used to model the thermodynamic behaviour of H_2O-CO_2 fluids. The solid solution models include carbonate minerals (Do; Holland and Powell, 1998), magnesite (Mag; Holland and Powell, 1998) clinopyroxene (Cpx; Holland and Powell, 1996), garnet (Grt; Holland and Powell, 1998), white mica (Phe; Auzanneau et al., 2010; Coggon and Holland, 2002), amphibole (Amp; Dale et al., 2005), ternary feldspar (Fuhram and Lindsley et al., 1988), K-feldspars (Kfs; Waldbaum and Thompson, 1968), biotite (Bio; Tajcmanová et al., 2009), and chlorite (Chl; Holland et al., 1998).

The numerical solutions have been computed using the Perple_X program MEEMUM (Connolly, 2005, 2009), which calculates free energy minimization as a function of specific environmental and compositional parameters and allows us to calculate stable assemblage at particular P-T conditions. This program has been used in combination with a custom-designed algorithm to model an open system.

2.4. CO_2 flux estimates

Estimates of CO_2 fluxes were obtained using the thickness (t_s) (Plank and Langmuir, 1998; Plank, 2014; Clift, 2017) and density (ρ_s) of sediment sequences entering each trench, and the speed of subduction (u_s) (van Keken et al., 2011). In our simulations, we consider a pressure step (ΔP) of 5 MPa, therefore, assuming a lithostatic pressure, the volume of sediment (V_s) within that variation of pressure, considering a unit metre length of arc, is:

$$V_s = \left(\frac{\Delta P}{\rho_s g} \cdot \frac{1}{\sin(\alpha)}\right) t_s \quad (1)$$

where α is the dip of the slab at each pressure step. The mass of the sediment (M_s) is the product of sediment volume and density that are assumed constant. We assume 3000 kg m^{-3} as representative density of sediments and AOC basalts at sub-arc depths. This assumption may promote a minor overestimation of CO_2 fluxes at shallower depths.

Assuming a speed of subduction u_s, the sediments remain within a 5 MPa range for a time ($\tau_{\Delta P}$):

$$\tau_{\Delta P} = \left(\frac{\Delta P}{\rho_s g} \cdot \frac{1}{\sin(\alpha)}\right) \cdot \frac{1}{u_s} \quad (2)$$

From our numerical results, we have derived the weight percent of CO_2 lost at each pressure step, and with our estimates of M_s and $\tau_{\Delta P}$ we can compute the CO_2 flux emitted every 5 MPa. Finally, to constrain the CO_2 flux from 1 to 5.5 GPa we quantify the total CO_2 flux emitted at fore-arc (1 to 2.3 GPa) and sub-arc (2.3 to 5.5 GPa)

Table 1
The estimates of the CO_2 flux emitted from subducting slabs and the measured CO_2 fluxes from arc volcanoes.

Subduction Trench	Metamorphic decarnonation of AOC basalts			Metamorphic decarbonation of sediments			Metamorphic decarbonation - Total	CO_2 flux from arc-volcanoes (a,b,c)
	Subducted inorganic CO_2 (Mt/yr)	CO_2 flux 1-2.3 Gpa (Mt/yr)	CO_2 flux 2.3-5.5 Gpa (Mt/yr)	Subducted inorganic CO_2 (Mt/yr)	CO_2 flux 1-2.3 Gpa (Mt/yr)	CO_2 flux 2.3-5.5 Gpa (Mt/yr)	CO_2 flux 2.3-5.5 Gpa (Mt/yr)	(Mt/yr)
Carbonate-poor lithologies								
Kamchatka (Kam)	1.06	0.00	0.89	0.53	0.00	0.53	1.43	1.55
Kurile (Kur)	1.05	0.00	0.80	0.05	0.00	0.05	0.85	0.71
Hokkaido (Hok)	0.89	0.00	0.68	0.17	0.00	0.17	0.85	0.09
Honshu-Japan (Hon)	1.16	0.00	0.37	0.22	0.00	0.22	0.60	0.15
Kyushu (Kyu)	1.05	0.00	1.05	0.04	0.00	0.04	1.09	0.68
Ryukyu (Ryu)	1.01	0.00	1.01	0.04	0.00	0.04	1.04	0.26
Sumatra (Sum)	1.33	0.00	1.33	0.76	0.00	0.76	2.08	0.57
Sunda Strait (SuS)	0.49	0.00	0.49	0.28	0.00	0.28	0.76	0.02
Java (Jav)	1.09	0.00	1.09	0.62	0.00	0.62	1.71	1.94
Ball/Lombok (BL)	1.16	0.00	1.15	0.68	0.00	0.68	1.83	0.72
Tonga (To)	2.20	0.01	0.57	0.21	0.00	0.21	0.78	0.09
Aleutians (Ale)	1.04	0.00	1.04	0.44	0.00	0.44	1.48	0.84
Alaska (Ala)	0.79	0.00	0.79	0.69	0.00	0.69	1.49	1.23
Cascadia (Cas)	0.36	0.36	0.00	0.05	0.05	0.00	0.00	0.38
Mexico (Mex)	1.68	1.68	0.00	0.13	0.13	0.00	0.00	3.92
Antilles (Ant)	0.20	0.00	0.20	0.20	0.00	0.20	0.41	0.71
North Chile (NC)	1.99	0.00	1.99	0.17	0.00	0.17	2.16	0.45
Central Chile (CC)	2.23	0.00	2.23	0.19	0.00	0.19	2.42	0.60
South Sandwich (SS)	0.75	0.00	0.75	0.25	0.00	0.25	1.00	0.12
Carbonate-rich lithologies								
Izu (Izu)	0.82	0.00	0.66	2.09	0.00	0.34	1.01	1.76
Marianas (Mar)	0.41	0.00	0.41	1.03	0.00	0.17	0.57	0.79
North Philippines (NPh)	1.72	0.00	1.72	15.60	0.00	2.16	3.88	0.82
South Philippines (SPh)	3.21	0.00	2.57	1.04	0.00	0.19	2.75	0.33
New Britain (NB)	1.83	0.00	1.05	4.53	0.00	1.23	2.27	3.28
Solomon Sol)	1.12	0.00	0.52	2.77	0.00	0.62	1.14	2.28
Vanuatu (Van)	3.43	0.01	3.42	5.49	0.00	2.05	5.47	7.49
New Zealand (NZ)	0.65	0.00	0.65	10.64	0.00	2.08	2.73	1.67
Guatemala-El Sal. (GES)	0.89	0.00	0.89	8.55	0.01	0.73	1.62	1.72
Nicaragua (Nic)	1.09	0.00	1.09	8.91	0.00	1.59	2.68	3.42
Costa Rica (CR)	0.47	0.00	0.47	4.21	0.00	0.74	1.20	1.26
Colombia-Ecuador (CE)	0.96	0.02	0.93	11.89	0.06	2.99	3.92	4.17
Peru (Per)	0.87	0.00	0.86	4.15	0.00	0.38	1.24	0.94
Calabria (Cal)	0.48	0.00	0.30	18.37	0.00	0.68	0.98	5.61
Total	39.49	2.11	31.99	105.00	0.26	21.47	53.46	50.57

Note: The estimates of the CO_2 flux emitted from subducting slabs reported here (as a result of the metamorphic decarbonation model) were calculated using the composition and thickness of each sediment lithology (Plank and Langmuir, 1998; Plank, 2014; Clift, 2017), the entire length of each arc sector and the subduction speed (van Keken et al., 2011) (Supplementary Table 1). CO_2 fluxes emitted from subducting AOC basalts through metamorphic decarbonation are calculated considering the upper basaltic portion (300 m of thickness) of the altered oceanic crust (Kelemen and Manning, 2015; Gorce et al., 2019; Merdith et al., 2019; Li et al., 2019). Metamorphic decarbonation along each subductiing slab was investigated using a typical hydrated and carbonated AOC basalt (Staudigel et al., 1989) (Supplementary Table 1). The CO_2 fluxes from arc volcanoes (persistent and diffuse degassing; Supplementary Table 2) were measured from previous studies conducted by [a]Burton et al. (2013), [b]Aiuppa et al. (2019) and [c]Werner et al. (2019).

depths (Table 1) through multiplying these per-metre outputs by the total length of the trench (Syracuse et al., 2010).

3. Results and discussion

3.1. The efficiency of decarbonation during subduction: the role of bulk composition and thermal regime

Our simulations of metamorphic decarbonation from different lithologies (sediments and AOC basalts) under different thermal regimes indicate that the proportion of CO_2 lost from subducting sediments decreases with increasing initial carbonate content (Fig. 3). Sediments such as siliceous ooze and carbonated clay with <10 vol.% of carbonate minerals (<5 wt.% CO_2 in the bulk composition) experience complete decarbonation beneath forearcs in subduction zones (with rarer high temperature pathways such as at Mexico and Cascadia) and beneath volcanic arcs for more common lower temperature subduction pathways (Fig. 4). In calcareous nannofossil oozes, chalks, and limestones, which contain more than 25 vol.% of carbonate minerals (12–34 wt.% CO_2), partial decarbonation occurs such that only 5 to 40% of their initial CO_2 is lost (Figs. 3 and 4). Therefore, 60 to 95% of the CO_2 subducted in these lithologies would be subducted to greater than 170 km depth, beyond where it could be incorporated into arc magma sources (Figs. 3 and 4a), a conclusion consistent with previous studies (Gorman et al., 2006; Kerrick and Connolly, 2001; Connolly, 2005; Thomsen and Schmidt, 2008; Thomson et al., 2016; Wong et al., 2019). These results highlight the importance of an arc-by-arc evaluation of slab CO_2 loss, as the fate of slab carbon depends on the arc-specific vol.% of carbonate minerals subducted and the subduction pressure-temperature pathway (Supplementary Fig. 1).

Our simulations indicate that metamorphic decarbonation from AOC basalts is 100% efficient in most of the subduction zones under intermediate and warm thermal regimes (Fig. 5; Table 1). Decarbonation is incomplete at sub-arc depths in the coldest subducting slab (Tonga, Solomon, Honshu, Hokkaido, Kuriles, Calabria and Kamchatka; Fig. 5; Table 1) and in three subduction zones with intermediate thermal regimes (Izu, South Philippines and New Britain). Thus, our results are consistent with the findings of Li et al. (2019) who proposed that altered oceanic crust may transport subducted carbon to the sites of diamond formation. We note that cold thermal regimes are more efficient in releasing CO_2 form carbonate-poor sediments than from AOC basalts (Figs. 4 and 5; Table 1). Intermediate thermal regimes can promote a complete

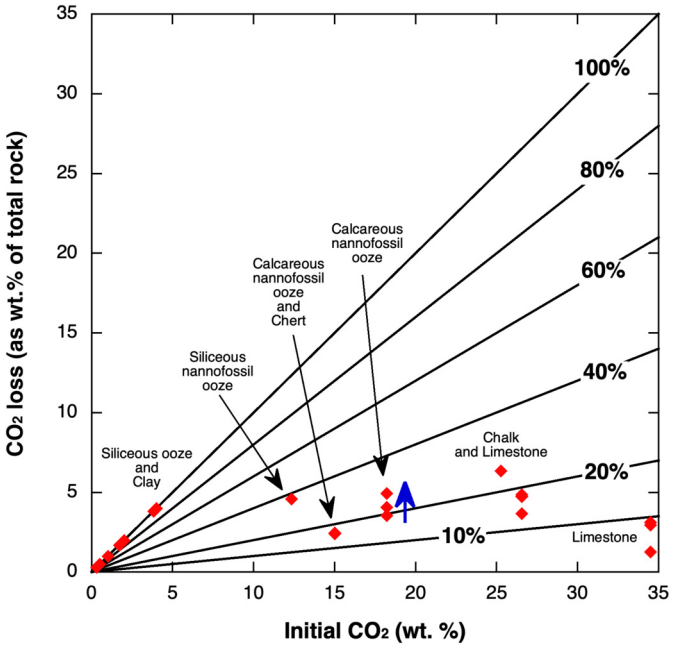

Fig. 3. Extent of CO_2 loss during metamorphic decarbonation. Bold black lines represent the percentage of CO_2 lost from carbonate-bearing sediments. Carbonated clay with a bulk composition containing <5 wt.% CO_2 (<10 vol.% of carbonate minerals) is representative of carbonate-poor sediments. Carbonate minerals within siliceous ooze and carbonated clay can be completely dissolved during subduction. Medium and rich carbonate lithologies, such as calcareous nannofossil ooze, chalk and limestones with a bulk composition containing 12–34 wt.% CO_2, are only partially dissolved during subduction. The blue arrow indicates an increase of the extent of CO_2 loss as a function of the thermal regime, which goes from a colder (Calabria) to a warmer (New Zealand) thermal regime.

decarbonation from AOC basalts and carbonate-poor sediments, and incomplete decarbonation from chalk and limestone. Decarbonation of sediments and AOC basalt occur at sub-arc depths under intermediate thermal regimes. Complete decarbonation of AOC basalts is observed beneath fore-arcs in warm subduction zones (Mexico and Cascadia) (Fig. 5; Table 1); this is similar to what we observed for carbonate-poor sediments in warm thermal regimes. We note that the approach of our model does not consider the transfer of CO_2 derived from AOC basalts to sediments. If we consider the scenario in which CO_2 released from basalts is transferred to carbonate-beating sediments, decarbonation may be slightly less efficient within carbonate-rich sediments (Fig. 3). Therefore, our model may overestimate the CO_2 flux released from the carbonate-rich sediments.

Under cold and intermediate thermal regimes, which account for 94% of the arcs considered here, our models indicate that metamorphic decarbonation of carbonate-bearing sediments and AOC basalt occurs mostly between ~80 and 170 km depth (~2.3 to 5.5 GPa) (Figs. 4 and 5; Table 1). This depth range corresponds to the zone beneath volcanic arcs, therefore, this CO_2 may be incorporated into the mantle wedge sources of arc magmas. Our models indicate that CO_2 is released in sharp pulses at fore- and sub-arc depths (Figs. 4b and 5b). Multiple decarbonation pulses may affect the timescale and efficiency of the CO_2 transfer from the slab to the surface.

Figs. 4b and 5b show that decarbonation occurs at lower pressures under warm thermal regimes and to gradually higher pressures under intermediate and cold thermal regimes. The calcareous nannofossil ooze models (with 18 wt.% CO_2; Fig. 3) demonstrate that warmer thermal regimes (e.g., New Britain) can generate greater CO_2 loss for a single bulk composition (as percentage of the bulk composition) than colder geothermal paths (e.g., Solomon and New Zealand) (Figs. 3 and 4a, b). This is also observed for subducting chalks and limestones (with ~25 wt.% CO_2; Fig. 3), where warmer thermal regimes such as Colombia-Ecuador can produce greater CO_2 loss than North Philippines, Nicaragua and Costa Rica (with the exception of South Philippines (Figs. 3 and 4a, b).

It is only under the warmest thermal regimes on Earth that metamorphic decarbonation of carbonate-poor sediments occurs at fore-arc depths (40–60 km depths), probably before the depth where CO_2 can be incorporated into arc magmas (Figs. 4b and 5b). Our results are consistent with the aforementioned geochemical findings for subducted carbonate-bearing rocks from the Aegean reported by Stewart and Ague (2020). Our modelling of 33 subduction zones concurs that metamorphic decarbonation is promoted at temperatures above 500 °C but such conditions are usually reached between 2.3 and 2.7 GPa under cold and intermediate thermal regimes, i.e. beneath the sites of arc magma genesis.

The approach of Syracuse et al. (2010) did not incorporate shear heating along the plate interface. We explored the consequence of adding reasonable levels of shear heating at the plate interface following van Keken et al. (2018) on metamorphic decarbonation We determined that shear heating only slightly affects the depths where decarbonation occurs. The quantitative effect on decarbonation is negligible (Supplementary Fig. 2). The lack of impact of shear heating is in part due to the inability of shear heating to significantly heat the slab interior even if the slab top is hotter (see, e.g., Figure 3 in van Keken et al., 2019).

3.2. Contribution of decarbonation on the deep carbon cycle: CO_2 transport from slab to surface

For each arc we can compare our modelled CO_2 flux from carbonate-bearing sediments and AOC basalts into the base of the mantle wedge with the volcanic CO_2 degassing output. Table 1 lists the CO_2 flux into the wedge over the 2.3–5.5 GPa pressure range for the entire length of each arc sector calculated from our model. If we assume that these margins are in a near steady-state then the CO_2 output flux produced by the volcanic arc (through persistent and diffuse degassing) should match this input flux, unless other processes of CO_2 loss or gain are in play. As noted in Aiuppa et al. (2019), current limits on gas monitoring probably do not capture entire arc CO_2 outputs. Furthermore, the carbonate abundance we measure in sediments today may be different from those currently breaking down under mantle wedges. Notwithstanding these limits we may gain insight into the global geological CO_2 cycle by comparing the input and output fluxes. We are helped by the fact that a large proportion of arc-CO_2 loss is from degassing volcanic systems whose fluxes have been measured or estimated. Therefore, we can test an initial steady-state hypothesis that the present-day CO_2 outputs (from the Aiuppa et al. (2019) and Werner et al. (2019) datasets) are balanced by the inputs from slab lithologies currently subducted under each margin. We do this by comparing the CO_2 lost from that sector by magmatic degassing to that supplied to each arc sector by metamorphic decarbonation of carbonate-bearing sediments and AOC basalts (Fig. 6a).

Fig. 6a shows that the correlation between CO_2 slab input and magmatic CO_2 output from several arcs cluster around and below the 1:1 line, while this correlation clusters above the 1:1 line only for a few subduction zones. This result supports the steady-state hypothesis and demonstrates that slab decarbonation processes followed by transport of CO_2 through the mantle wedge melting zone to magmatic systems have the potential to play an important role in controlling the magnitude of arc CO_2 degassing in most of the subduction zone.

In some subduction zones the input of CO_2 into the mantle wedge from carbonate-bearing sediments and AOC basalts exceeds the arc output (i.e. those arcs that plot below the 1:1 line in Fig. 6a), while in others the volcanic CO_2 output exceeds that

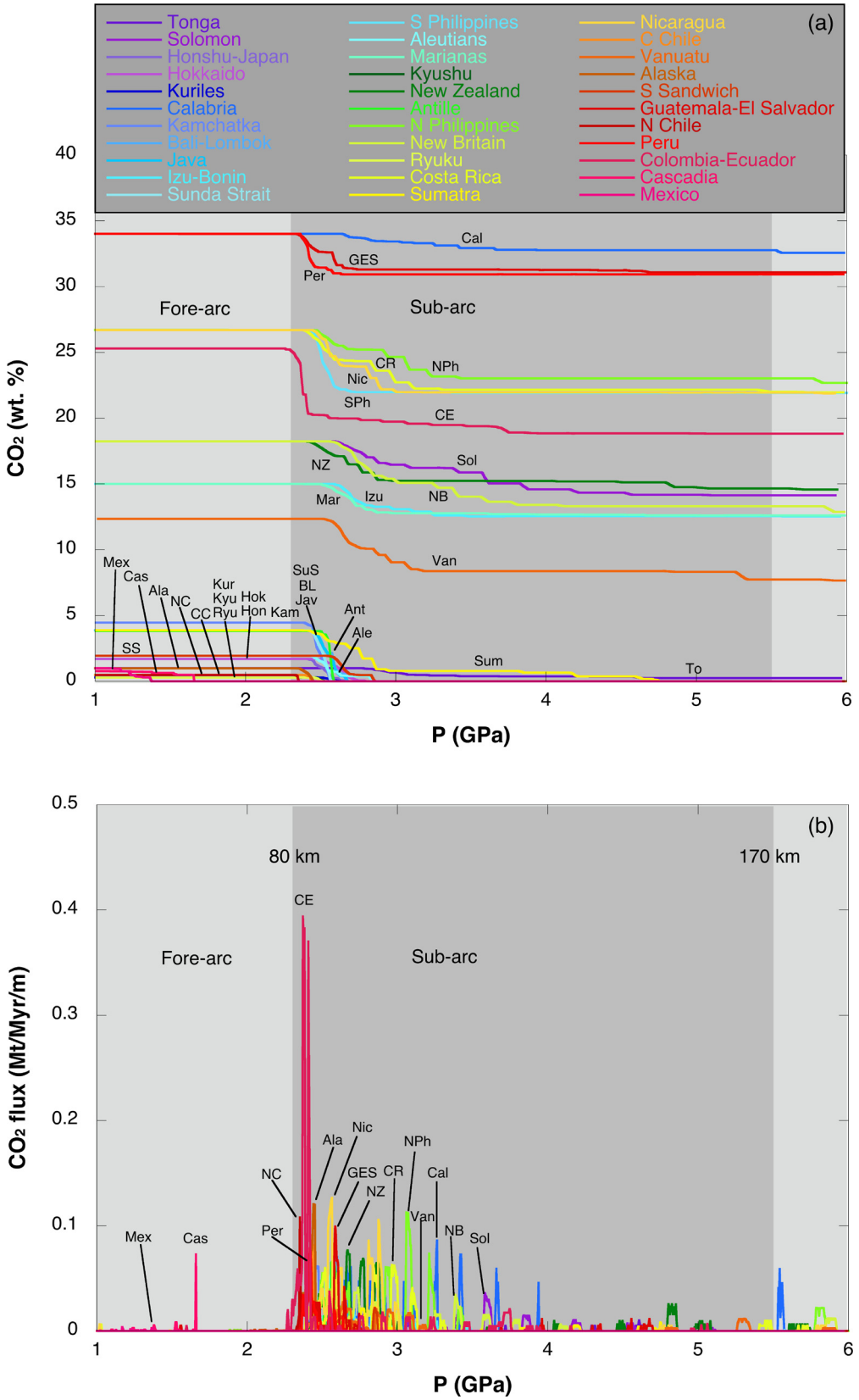

Fig. 4. Metamorphic decarbonation of carbonate-bearing sediments in 33 subduction zones. We used representative sediment compositions (Supplementary Table 1) for the subduction zones investigated. Decarbonation trend (a) and CO_2 fluxes (b) as function of depth in each subduction zone. The hottest subduction zones (Mexico and Cascadia) are fully decarbonated in the fore-arc. The rest of the subducting slabs with colder thermal regimes than Mexico and Cascadia lose significant CO_2 between ~2.3 and 5.5 GPa (between ~80 and 170 km depth). See Table 1 for abbreviations. Estimates of the CO_2 flux (Table 1), reported here (b), were calculated using the thickness of each sediment lithology (Plank and Langmuir, 1998; Plank, 2014; Clift, 2017) and the speed of subduction (van Keken et al., 2011). The subduction zone colours are coded by slab temperature considering the temperature at 100 km depth within the sediments (van Keken et al., 2011). (For interpretation of the colours in the figure(s), the reader is referred to the web version of this article.)

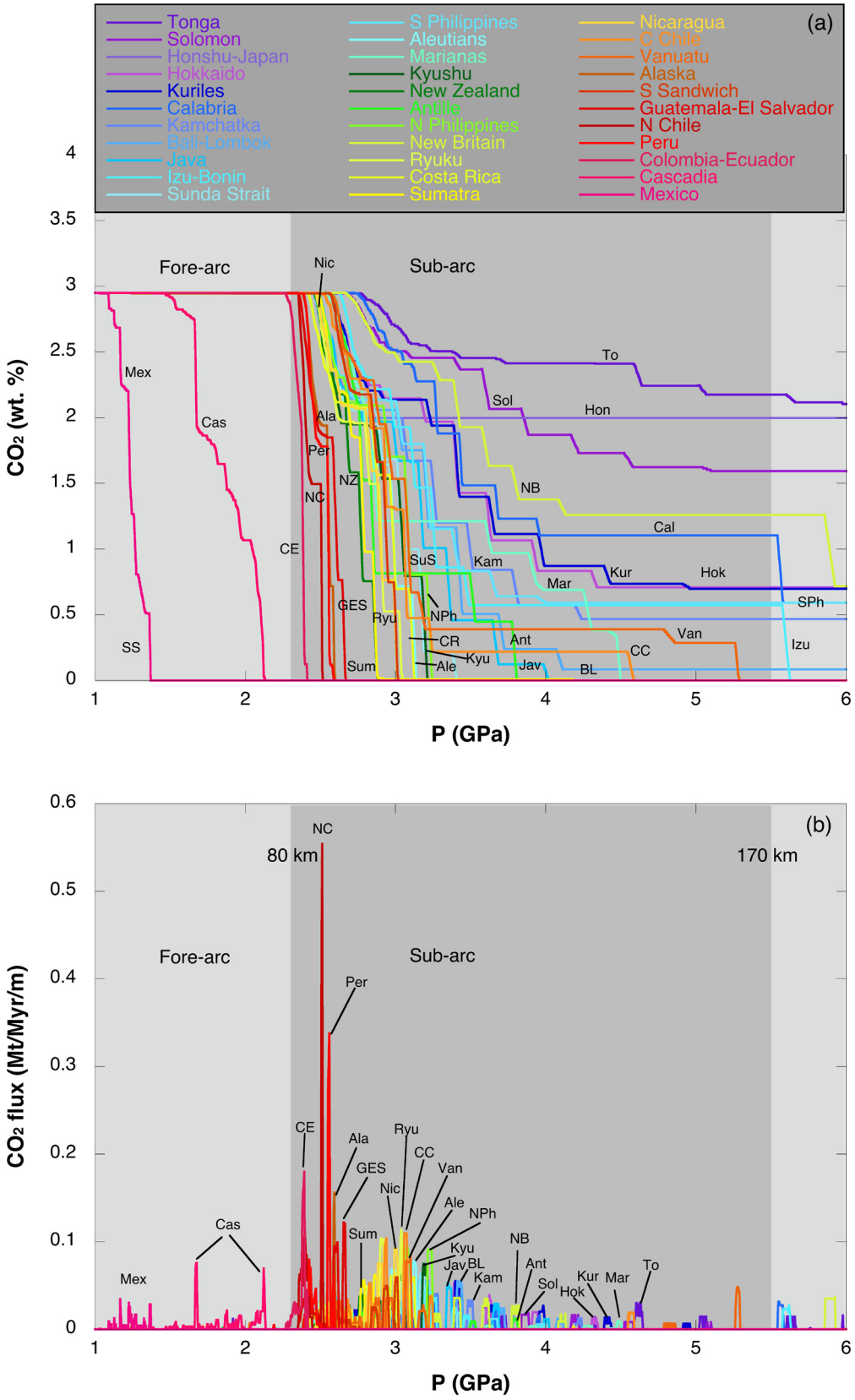

Fig. 5. Metamorphic decarbonation of carbonated AOC basalts in 33 subduction zones. The simulations of the 33 subducting slabs were performed using a representative AOC basalt (Supplementary Table 1). Decarbonation trend (a) and CO_2 fluxes (b) as function of depth in each subduction zone. See Table 1 for abbreviations. Estimates of the CO_2 flux (Table 1), reported here (b), were calculated using a thickness of 300 m and the speed of subduction (van Keken et al., 2011). (For interpretation of the colours in the figure(s), the reader is referred to the web version of this article.)

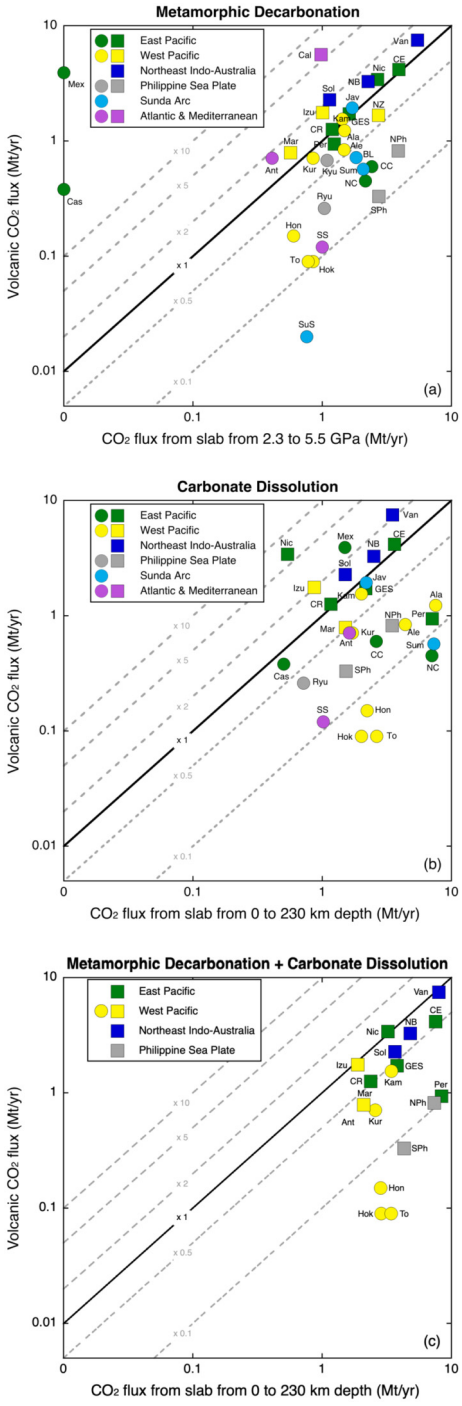

Fig. 6. Comparison of CO_2 released from volcanic arcs (Aiuppa et al., 2019; Werner et al., 2019) with the CO_2 input from sub-arc slab. (a) The CO_2 input from sub-arc slab obtained through metamorphic decarbonation. (b) The CO_2 input from slab between 0 and 230 km depth obtained through carbonate dissolution (Farsang et al., 2021). (c) The CO_2 input from slab between 0 and 230 km depth obtained through the combination of metamorphic decarbonation and carbonate dissolution (Farsang et al., 2021). Only the subducting slabs in which metamorphic decarbonation is not 100% efficient in liberating CO_2 at fore- and sub-arc depths are considered in the panel (c), as carbonate dissolution may be more efficient at sub-arc depths (Galvez et al., 2016; Farsang et al., 2021); so metamorphic decarbonation and dissolution might occur together at sub-arc depths. Circles: Subduction of low-carbonate sediments. Squares: Subduction of high-carbonate sediments. Inclined lines illustrate the magnitude of the volcanic output compared to the sub-wedge input of CO_2. Colour indicates geographic region: Green - subduction of East Pacific lithosphere; Yellow - subduction of West Pacific lithosphere; Dark blue - subduction of Northeast Indo-Australian lithosphere; Grey - subduction of Philippine Sea Plate lithosphere; Pale blue - subduction of North Indian-Australia lithosphere (Sunda Arc); Fuchsia - subduction of Atlantic or Mediterranean lithosphere. See Table 1 for abbreviations.

which we have modelled being added to the wedge from sediment and AOC basalts (i.e. those arcs that plot above the 1:1 line in Fig. 6a). We observe a general tendency for carbon-rich (squares) or carbon-poor (circles) sediments and AOC basalts to lead to one or the other of these situations. We observe that volcanic CO_2 outputs exceed in some subduction zone with carbonate-rich sediments (e.g., Calabria, Solomon, Izu). This result indicates that metamorphic decarbonation of chalk and limestone, in addition to the CO_2 lost from AOC basalts, may be not efficient in liberating enough CO_2 from the slab under cold thermal regimes to balance the arc volcanic CO_2 emissions. In general, we observe that there are no excess volcanic CO_2 emissions in the majority of subduction zones with carbonate-poor sediments (Fig. 6a); this indicates that metamorphic decarbonation of AOC basalts and clay could liberate sufficient CO_2 from the slab to balance the arc volcanic CO_2 outputs. The exceptions are Cascadia and Mexico that are displaced above the 1:1 line, as volcanic CO_2 outputs exceed the CO_2 slab input at sub-arc depths.

The results discussed in our study on carbon mobilization and transport from the slab to the surface should be contextualized considering that in our decarbonation model we assume oxidizing conditions (Debret and Sverjensky, 2017). However, the redox state of subducting slabs may differ widely (Galvez et al., 2013; Debret and Sverjensky, 2017). For instance, reduced fluids may react with carbonate minerals that can favour their saturation in carbon leading to precipitation of graphite (Galvez et al., 2013). This may affect the mobilization and transport of subducting carbon, hindering carbon recycling to the surface. Rock-carbonation by fluid–rock interactions may also have an important impact on the direct transfer of carbon to the mantle wedge, providing a mechanism to stabilize and retain a part of the total carbon within a subducting slab (Piccoli et al., 2016).

The rate of water flow within the slab also affects carbon mobilization. It has been demonstrated thermodynamically that pervasive flow promotes greater mobilization of carbon than channelized flow from the slab to the mantle wedge (Gorman et al., 2006). Plümper et al. (2017) also show that both pervasive and channelized water flows occur within the slab, but that pervasive flow is considered subordinate to channelization. In order to consider a scenario in which the water flow is faster we increased the transport rate by a factor of 100 (from 0.25 m yr^{-1} to 25 m yr^{-1}; Wilson et al., 2014). By increasing the water flow velocity within the AOC basalts and sediments, we provide less H_2O to the system that will be accounted for by the metamorphic solid-solution reactions. This approach allows us to consider only a percentage of the water supplied by the slab serpentinization (van Keken et al., 2011) for the equilibrium. Despite the transport rate increases by a factor of 100, thus reducing the H_2O available for the metamorphic solid-solution reactions, decarbonation is still efficient considering fast transport rates (Supplementary Table 3). This indicates that decarbonation remains an important process in releasing CO_2 from the slab even if the amount of H_2O available for metamorphic reactions is reduced by faster transport rates.

3.2.1. Comparison between metamorphic decarbonation and carbonate dissolution

Our thermodynamic model considers only CO_2 mobilisation into the mantle wedge by metamorphic decarbonation. Carbonate dissolution (Frezzotti et al., 2011; Ague and Nicolescu, 2014; Kelemen and Manning, 2015; Galvez et al., 2016; Farsang et al., 2021) and melting (Poli, 2015; Mann and Schmidt, 2015) may also mobilise CO_2. It has been shown that carbonate melting will not occur in cool and medium temperature subduction pathways (Mann and Schmidt, 2015) and, therefore, we do not consider carbonate melting in our modelling. Carbonate dissolution is an important mechanism for carbon removal up to sub-arc depths in

several subduction zones (Kelemen and Manning, 2015; Galvez et al., 2016; Farsang et al., 2021). We compare our results obtained from metamorphic decarbonation with the results obtained from Farsang et al. (2021) on carbonate dissolution below. This comparison helps us to better understand the potential contribution of both the processes in liberating CO_2 from the slab to the mantle wedge in different subduction zones on Earth (Fig. 6a, b). This also provides insights into other potential processes that might release CO_2 between the mantle wedge and the surface. These processes include diapirism of sediments intruding into the mantle wedge, in which CO_2 from the slab may be added by assimilation of these sediments (e.g., Chen et al., 2021) and assimilation of carbon from the lithosphere (Deegan et al., 2010; Troll et al., 2012; Carter and Dasgupta, 2015; Aiuppa et al., 2017).

Fig. 6b compares the CO_2 that Farsang et al. (2021) determined may be supplied to each arc sector by carbonate dissolution of carbon-bearing sediments (inorganic and organic carbon) and AOC basalts with the CO_2 lost from that sector by magmatic degassing (Aiuppa et al., 2019; Werner et al., 2019). Farsang et al. (2021) considered carbonate dissolution at fore- and sub-arc depths (to 230 km depth), although the main contribution is obtained at sub-arc depths (Fig. 6b). Fig. 6b shows that in subduction zones with carbonate-poor sediments, with the exception of Mexico, volcanic CO_2 outputs do not generally exceed the inputs. However, in several subduction zones with carbonate-rich sediments (chalk and limestones) carbonate dissolution does not produce enough CO_2 from the slab to balance the arc volcanic CO_2 emissions (Fig. 6b). These results are broadly similar to our results obtained considering metamorphic decarbonation (Fig. 6a). Most of the water is released from the slab at sub-arc depths (van Keken et al., 2011), therefore decarbonation and dissolution might occur at the same depths in liberating CO_2. For this reason, we combine fluxes produced by metamorphic decarbonation and mineral dissolution and we compare to fluxes at arcs where either process on their own is insufficient to explain the arc fluxes (e.g., Solomon, New Britain, Vanuatu, Nicaragua, Colombia-Ecuador, Izu, Marianas) (Fig. 6c). Metamorphic decarbonation can be efficient at fore- and sub-arc depths depending on the P-T path (Figs. 4 and 5), while carbonate dissolution may be more efficient at deeper depths such as sub-arc depths (Galvez et al., 2016; Farsang et al., 2021). Therefore, if metamorphic decarbonation is not efficient at fore-arc depths, it is possible that decarbonation and dissolution might occur at sub-arc depths. Particularly, if metamorphic decarbonation is not 100% efficient in liberating CO_2 from the subducting slab at sub-arc depth, dissolution may release the rest of the CO_2 within sediments and AOC basalts (Fig. 6c). We highlight that whether these two processes can operate at the same time and whether the operation of one affects the efficiency of the other is under debate. It is likely that the interaction between decarbonation and dissolution is very complicated because decarbonation will change the activity of CO_2 and H_2O in the fluid, which will affect dissolution and vice versa. This implies that the increased CO_2 activity and decreased H_2O activity will decrease the efficiency of both processes, therefore, the combined CO_2 fluxes released from slabs reported in Fig. 6c are maximum fluxes. This suggests that the combined effects of metamorphic decarbonation and carbonate dissolution together may produce sufficient decarbonation to explain arc volcanic CO_2 outputs in subduction zones with carbonate-rich sediments (Fig. 6c).

Previous studies suggested that diapirism of buoyant sediment into the mantle wedge may provide a reservoir from which carbonate can be assimilated during ascent of arc magma, thus contributing to the carbon flux in volcanic arcs (Kelemen and Manning, 2015; Chen et al., 2021). Furthermore, assimilation of carbon from the lithosphere (magma-carbonate interaction) may be invoked to explain the difference between CO_2 input and output (Carter and Dasgupta, 2015; Aiuppa et al., 2017). A more detailed discussion is provided below to understand the controls on CO_2 fluxes and the contribution of metamorphic decarbonation. We first consider subduction zones on a geographic basis.

3.2.2. East Pacific

Most of the East Pacific subduction zones with carbonate-rich sediments (Columbia-Ecuador, Nicaragua, Guatemala-El Salvador, Costa Rica and Peru) plot close to the 1:1 line, implying that the CO_2 flux produced through decarbonation of sediment and AOC basalts can balance the volcanic outputs (Fig. 6a). This indicates that decarbonation may be an important process for the deep carbon cycle in these subduction zones. This is in agreement with previous studies, based on gas geochemistry, which suggest that decarbonation of subducting carbonate-rich sediments and AOC basalts may provide an important contribution in balancing the output from the arcs (Sano and Marty, 1995; Hilton et al., 2002; Shaw et al., 2003). We note that our model does not predict fore-arc decarbonation along the Costa Rica slab, which is in contrast with recent gas geochemistry studies (Shaw et al., 2003; Barry et al., 2019). Similar results can be observed in the scenario in which carbonate dissolution dominates the CO_2 liberation from the slab (Fig. 6b), with the exception of Nicaragua that plot more markedly above the 1:1 line.

CO_2 fluxes emitted from the slabs of North and Central Chile greatly exceed the volcanic emissions (Fig. 6a), which suggests that decarbonation can account for the entire volcanic output while transport of carbon to the surface may not be efficient and direct. This result corroborates evidence that the mantle wedge contains fluids transferred from the subducted lithosphere (Hickey-Vargas et al., 2002). We observe the same result if we consider the scenario in which the CO_2 fluxes of the Chilean segments are produced by carbonate dissolution (Fig. 6b). Therefore, CO_2 may be sequestered as carbonated rocks (Sieber et al., 2018) somewhere into the mantle wedge or arc lithosphere over long time scales (Hickey-Vargas et al., 2002).

Our models indicate that the Mexican and Cascadian slabs are sufficiently warm to purge most of their CO_2 before reaching 2.3 GPa. We have plotted these with a nominal slab input for comparative purposes, which makes clear that their volcanic CO_2 fluxes are far in excess of our model predictions (Fig. 6a). Mexico's 3.92 Mt/yr volcanic flux is also large compared to the majority of other arcs and is all the more notable for being mostly generated by a single volcano, Popocatépetl, which emits more CO_2 than any other terrestrial volcano (Aiuppa et al., 2019; Werner et al., 2019). Therefore, our model indicates that metamorphic decarbonation of the carbonate-bearing sediments and AOC basalts subducted beneath Mexico is not a viable source for the high CO_2 flux from Popocatépetl. The scarce efficiency of carbonate dissolution (Fig. 6b) along the Mexican slab (Farsang et al., 2021) indicate that dissolution is also not the process that promotes the high CO_2 flux from Popocatépetl. Previous studies suggested that the prodigious CO_2 flux from Popocatépetl should result from magma assimilation of limestone in the upper crust (Schaaf et al., 2005; Carter and Dasgupta, 2015; Aiuppa et al., 2017). Likewise, our results also indicate that metamorphic decarbonation cannot be the dominant process supplying CO_2 to the warm and complementary Cascadian arc (Figs. 4 and 5). Dissolution of inorganic and organic carbonate (Farsang et al., 2021) may be the dominant process along this warm slab (Fig. 6b). However, if all CO_2 in the sediments and AOC basalts is lost via metamorphic decarbonation at the fore-arc depths (Figs. 4 and 5), which means that by the time the slab reaches sub-arc depths it is essentially CO_2 free and there should be no inorganic carbonate available for dissolution at sub-arc depths. Therefore, organic carbonate could be the source for the Cascadian volcanic arc CO_2 emissions. These findings are supported by a field-based studies in an exhumed slab

from Greece which found that between 40 and 65 vol.% of the CO_2 in subducted sediments may be released into a fore-arc at ~500 °C (warm slab) via carbonate mineral dissolution (Ague and Nicolescu, 2014) and metamorphic decarbonation reactions (Stewart and Ague, 2020). The scenario offered by Mexico and the Cascadian, on the one hand, and the other eastern Pacific subduction zones, on the other hand, provides a framework to understand patterns of CO_2 input and output in many other convergent margins in the Atlantic, Mediterranean and Indian oceans.

3.2.3. West Pacific

Our modelled CO_2 input from subducted sediment and AOC basalts exceeds or equals the CO_2 emitted by western Pacific arcs in most of the cases except for Izu and Marianas (Fig. 6a). This is especially true of Kamchatka, Kurile, Hokkaido, Honshu, Tonga, Aleutians, Alaska and New Zealand. This result is supported by studies based on gas geochemistry, which indicate that the initial subducted carbon, dominantly sourced from AOC basalts (particularly Kurile and Kamchatka as reported by Fischer et al., 1998 and Hilton et al., 2002) and sediment, is mostly lost from the slab during metamorphic decarbonation at sub-arc depth (Sano and Marty, 1995; Hilton et al., 2002; Lopez et al., 2017; Epstein et al., 2021). The low volcanic CO_2 output may be a sampling artefact, since some of the volcanic outputs data rely on arcs that are (geographically or bathymetrically) remote and difficult to sample or where the current volatile output may not capture historic highs. Sequestration of CO_2 may also occur into the mantle wedge or arc lithosphere, which can prevent the transport of COH fluids through volcanic arcs. Nevertheless, the overall impression is that most of these arcs emit a relatively low proportion of the CO_2 that our models suggest is transferred from subducted sediments and AOC basalts to their mantle wedges. The exceptions are Izu and Marianas, as their volcanic CO_2 outputs exceed the slab-derived CO_2, therefore, subducted sediments and AOC basalts may be not the main source of the CO_2 emitted from Izu and Marianas volcanic arcs (e.g., Macpherson et al., 2010).

3.2.4. Northeast Indo-Australia and Philippine Sea Plate

The volcanic CO_2 output of the northeast Indo-Australia Plate, including the Solomon microplate, slightly exceeds the input of sedimentary and AOC basaltic CO_2 indicated by our decarbonation models while Vanuatu and New Britain plot close to the 1:1 line (Fig. 6a). The arc lithosphere in these subduction zones (Vanuatu, New Britain, and Solomon) is geologically young and does not host large deposits of sedimentary carbonate. Therefore, upper plate crustal contamination cannot be invoked as a substantial source of the excess CO_2 emitted from these arcs. Likewise, carbonate dissolution also fails to generate sufficient CO_2 from the slabs to account for the volcanic outputs and so can be considered an important source of volcanic carbon (Fig. 6b), but not the unique one. Therefore, we consider the slab derived CO_2 fluxes obtained from the combination of metamorphic decarbonation and carbonate dissolution (Fig. 6c), which implies that the two processes together can occur efficiently at sub-arc depths. The combination of decarbonation and dissolution can equal the CO_2 emitted by northeast Indo-Australia volcanic arcs (Fig. 6c). This suggests that the volcanic CO_2 output of the northeast Indo-Australia volcanic arcs may be fed by decarbonation and carbonate dissolution along subducting slabs at sub-arc depths.

CO_2 fluxes emitted from the slabs of the Philippines Sea plate exceed volcanic emissions (Fig. 6a). Regarding the Kyushu, Ryukyu and South Philippine arcs, decarbonation of carbonated AOC basalts provides the main contribution to the CO_2 released from their slabs into the mantle wedge. At these margins older oceanic lithosphere is subducted than at the Vanuatu, New Britain, and Solomon margins. Since secondary carbonate appears to build up in oceanic crust in the few million years after accretion (Li et al., 2019), the older altered oceanic crust in these subduction zones could contribute more CO_2 than slabs feeding the northeast Indo-Australian arcs. The imbalance between the input and output of CO_2 in the arcs of the Philippines Sea plate suggests that CO_2 may be accumulated and stored into the mantle wedge or arc lithosphere before to reach the surface. This observation is also supported from the scenario in which carbonate dissolution was the main process in liberating CO_2 from the slab (Fig. 6b).

3.2.5. Sunda Arc

Metamorphic decarbonation of sediments and AOC basalts is an important process that may explain the Javan volcanic emissions (Fig. 6a). Carbonate dissolution may also provide an important contribution to balance the Javan volcanic outputs (Fig. 6b). Assimilation of crustal carbonate has been proposed as a further source of the emissions (Deegan et al., 2010; Troll et al., 2012; Aiuppa et al., 2017). In the Sumatra and Bali-Lombok sectors our estimate of how much CO_2 is added to the mantle wedge is slightly larger than their volcanic outputs (Table 1; Fig. 6a). Therefore, decarbonation of subducting sediments and AOC basalts may be the principal source of CO_2 emitted from these two sectors, which is also consistent with the findings of carbon isotope and $CO_2/^3He$ studies (Poorter et al., 1991; Varekamp et al., 1992; Halldorsson et al., 2013). Results reported from Farsang at el. (2021) indicate that carbonate dissolution may also have an important role in recycling carbon from the Sumatra subducting slab (Fig. 6b). This suggests that decarbonation and/or dissolution may be important processes in liberating CO_2 from the Sumatra slab. The volcanic CO_2 output from the Sunda Straight can be comfortably accounted for by sediment and AOC basalt input (Fig. 6a). Indeed, at face value the low volcanic output in Sumatra, Bali/Lombok, and Sunda Straight may indicate substantial carbon sequestration in the mantle wedge.

3.2.6. Atlantic

In the Atlantic, less CO_2 is released from the South Sandwich Arc than is added to its mantle wedge, similar to the situation in the majority of other subduction zones with carbonate-poor sediments of the East and West Pacific, northeast Indo-Australia, Philippines Sea Plate, and Sunda arc. In contrast, the volcanic CO_2 output from the Lesser Antilles Arc is almost two times higher than the CO_2 input we determined from decarbonation of subducted sediments and AOC basalts (Fig. 6a). Despite decarbonation being 100% efficient and dominantly occurring at sub-arc depth in the Lesser Antilles Arc (Table 1; Figs. 4 and 5), as also observed by Li et al. (2020), it cannot be the unique process in liberating CO_2 from the slab. Only inorganic carbon is considered in our decarbonation model, but we note that organic carbon is abundant in the sediments of Lesser Antilles (Clift, 2017) and carbonate dissolution mobilizes organic (reduced) carbon from this slab (Farsang et al., 2021). Therefore, the contribution of carbonate dissolution might balance the volcanic CO_2 output from the Lesser Antilles Arc (Fig. 6b). Assimilation of crustal sediments is also a widely documented process in the geochemical evolution of Antilles magmatism (Davidson, 1987; Bezard et al., 2015) and recent tectonic models have strengthened the case for this sediment residing in the upper plate (Allen et al., 2019). Prior geochemical modelling of Lesser Antilles magmatism has focused on assimilation of clastic sediment but the excess CO_2 arc emissions relative to our model suggests there may also be a potential remobilisation of upper plate carbonate-bearing sediments (Davidson, 1987).

3.2.7. Calabria

The Calabrian margin subducts Mesozoic oceanic crust of the Ionian Sea (Piana Agostinetti et al., 2009; Polonia et al., 2011), while its accretionary wedge comprises Plio-Quaternary units and

Messinian evaporites overlying Tertiary and Mesozoic sediments (Cernobori et al., 1996; Polonia et al., 2011). The Mesozoic carbonates comprise approximately 2000 m of limestone (Polonia et al., 2011) that lies on the underlying oceanic crust (Piana Agostinetti et al., 2009). Detachments in the accretionary wedge occur at the base of the Messinian evaporites and at the top of the Mesozoic carbonates, therefore, the Mesozoic limestones have the highest probability of subduction with the oceanic crust (Piana Agostinetti et al., 2009; Polonia et al., 2011). To investigate how subduction of carbonate-bearing sediment and AOC basalts contributes to the CO_2 fluxes emitted from Aeolian volcanoes and Etna, we assumed that the slab beneath Calabria is able to transport 1000 m of limestones to sub-arc depths and 300 m of carbonated AOC basalts (Supplementary Table 1). Our model indicates that in total, considering decarbonation of limestones and AOC basalts, 0.98 Mt/yr CO_2 can be released in the mantle at sub-arc depths. The estimate obtained with our decarbonation model is insufficient to account for the volcanic flux from the Calabria volcanoes (Etna, Stromboli, and Vulcano combined; Table 1; Fig. 6a). Our results indicate that decarbonation of limestones and AOC basalts may be one of the important sources of CO_2 that contribute to the high volcanic output of Calabria, which is consistent with the $CO_2/^3He$ ratios and estimated sources of carbon in gas and fluids from Vulcano (Sano and Marty, 1995). Our results are also consistent with Tonarini et al. (2001), who proposed that the altered Ionian oceanic crust and its sedimentary cover are the sources of the fluids contaminating the mantle source of Mt. Etna magmas. However, this would require some portion of the volcanic CO_2 be derived from other sources. Etna gases are characterized by unusually high CO_2/S, which have been attributed to magma-limestone interactions in the upper crust (Aiuppa et al., 2017, 2019). We suggest that a proportion of the CO_2 emitted from Etna is fed by decarbonation of subducting limestones and AOC basalts but that this is augmented by CO_2 liberated by magma-crust interaction. Furthermore, the role of carbonate dissolution in the Calabrian slab has not been investigated, but it may be an important CO_2 source that could be studied in future works.

4. Conclusion

Our study investigates the potential contribution of metamorphic decarbonation on the deep carbon cycle considering 33 subduction zones. A key result of our study is that the pervasive hydration of subducted sediments promotes intense sub-arc metamorphic decarbonation of carbonate-bearing sediments and AOC basalts, under cold and intermediate thermal regimes, directly beneath the observed locations of arc volcanism. Metamorphic decarbonation of AOC basalts is not 100% efficient under cold thermal regimes. The warmest slabs on Earth (Cascadia and Mexico) promote metamorphic decarbonation of carbonate minerals at fore-arc depths. Our modelling shows also that all of the CO_2 in carbon-poor lithologies is likely to be mobilized and lost from the slab. In contrast, the CO_2 from carbonate-rich lithologies, such as calcareous nannofossil ooze, chalk, and limestone, is only partially mobilized via decarbonation. Dissolution of inorganic and organic carbon (Kelemen and Manning, 2015; Farsang et al., 2021) is the other process that has been proposed to play an important role in liberating CO_2 from the slab. Both metamorphic decarbonation or carbonate dissolution by itself can liberate sufficient CO_2 from carbonate-rich lithologies (calcareous nannofossil ooze, chalk and limestones) to balance volcanic CO_2 outputs for some arcs. The efficient occurrence of metamorphic decarbonation and carbonate dissolution together at sub-arc depths is needed to equal the CO_2 emitted by, for instance, northeast Indo-Australia, Nicaragua and Izu-Bonin volcanic arcs. We propose that the combination of decarbonation and dissolution is the best explanation for high CO_2 emissions from carbonate-rich subduction zones in Calabria, Nicaragua, Colombia-Ecuador, Vanuatu, New Britain, Solomon, Izu and Marianas. This is also applicable to some subduction zones with carbonate-poor sediments such as Lesser Antilles, Cascadia and Mexico.

Assimilation of carbon from the lithosphere may also contribute to the strong CO_2 emission of Popocatépetl in Mexico. We observe that slab-derived CO_2 exceeds the volcanic CO_2 emissions in subduction zones with carbonate-poor sediments. This suggests that the mantle wedge or arc lithosphere may accumulate and store CO_2. The mantle wedge and lithosphere of any active arc may be dynamic reservoirs in which magmatism may add and remove multiple generations of CO_2 at multiple levels. The pathways and processes by which this occurs are still difficult to investigate. Further modelling and experimental investigations are required to elucidate the fluid transfer processes within the mantle wedge.

CRediT authorship contribution statement

Fabio Arzilli: Conceptualization, Data curation, Formal analysis, Investigation, Methodology, Software, Supervision, Validation, Visualization, Writing – original draft. **Mike Burton:** Conceptualization, Funding acquisition, Investigation, Methodology, Project administration, Resources, Supervision, Visualization, Writing – original draft. **Giuseppe La Spina:** Data curation, Formal analysis, Methodology, Software, Validation, Writing – review & editing. **Colin G. Macpherson:** Conceptualization, Data curation, Investigation, Methodology, Resources, Supervision, Visualization, Writing – original draft. **Peter E. van Keken:** Methodology, Resources, Software, Writing – review & editing. **Jamie McCann:** Formal analysis, Validation, Writing – review & editing.

Declaration of competing interest

The authors declare that they have no known competing financial interests or personal relationships that could have appeared to influence the work reported in this paper.

Data availability

Data will be made available on request.

Acknowledgements

We gratefully acknowledge funding support from RCUK NERC DisEqm project (NE/N018575/1). The research leading to these results has received funding from the European Research Council under the European Union's Seventh Framework Programme (FP/2007-2013) / ERC Grant Agreement n. 279802. We are grateful to P. Bouilhol and J. A. D. Connolly for helpful advice on Perple_X software. We thank B. McCormick Kilbride and M. W. Schmidt for stimulating and helpful discussions. We thank Prof. Craig Manning and other anonymous reviewers for providing thorough reviews that greatly improved the quality of our paper.

Appendix A. Supplementary material

Supplementary material related to this article can be found online at https://doi.org/10.1016/j.epsl.2022.117945.

References

Abers, G.A., van Keken, P.E., Hacker, B.R., 2017. The cold and relatively dry nature of mantle forearcs in subduction zones. Nat. Geosci. 10, 333–337. https://doi.org/10.1038/ngeo2922.

Abers, G.A., van Keken, P.E., Wilson, C.R., 2020. Deep decoupling in subduction zones: observations and temperature limits. Geosphere 16, 1408–1424. https://doi.org/10.1130/GES02278.1.

Ague, J.J., Nicolescu, S., 2014. Carbon dioxide released from subduction zones by fluid-mediated reactions. Nat. Geosci. 7, 355–360. https://doi.org/10.1038/NGEO2143.

Aiuppa, A., Fischer, T.P., Plank, T., Robidoux, P., Di Napoli, R., 2017. Along-arc, inter-arc and arc-to-arc variations in volcanic gas CO_2/S_T ratios reveal dual source of carbon in arc volcanism. Earth-Sci. Rev. 168, 24–47. https://doi.org/10.1016/j.earscirev.2017.03.005.

Aiuppa, A., Fischer, T.P., Plank, T., Bani, P., 2019. CO_2 flux emissions from the Earth's most actively degassing volcanoes, 2005–2015. Sci. Rep. 9, 1–17. https://doi.org/10.1038/s41598-019-41901-y.

Allen, R.W., Collier, J.S., Stewart, A.G., Henstock, T., Goes, S., Rietbrock, A., VoiLA Team, 2019. The role of arc migration in the development of the Lesser Antilles: a new tectonic model for the Cenozoic evolution of the eastern Caribbean. Geology 47, 891–895. https://doi.org/10.1130/G46708.1.

Alt, J.C., Schwarzenbach, E.M., Früh-Green, G.L., Shanks III, W.C., Bernasconi, S.M., Garrido, C.J., Crispini, L., Gaggero, L., Padrón-Navarta, J.A., Marchesi, C., 2013. The role of serpentinites in cycling of carbon and sulfur: seafloor serpentinization and subduction metamorphism. Lithos 178, 40–54. https://doi.org/10.1016/j.lithos.2012.12.006.

Auzanneau, E., Schmidt, M.W., Vielzeuf, D., Connolly, J.D., 2010. Titanium in phengite: a geobarometer for high temperature eclogites. Contrib. Mineral. Petrol. 159, 1–24. https://doi.org/10.1007/s00410-009-0412-7.

Barry, P.H., de Moor, J.M., Giovannelli, D., Schrenk, M., Hummer, D.R., Lopez, T., Pratt, C.A., Segura, Y.A., Battaglia, A., Beaudry, P., Bini, G., Cascante, M., d'Errico, G., Di carlo, M., Fattorini, D., Fullerton, K., Gazel, E., González, G., Halldórsson, S.A., Iacovino, K., Ilanko, T., Kulongoski, J.T., Manini, E., Martínez, M., Miller, H., Nakagawa, M., Ono, S., Patwardhan, S., Ramírez, J., Regoli, F., Smedile, F., Turner, S., Vetriani, C., Yücel, M., Ballentine, C.J., Fischer, T.P., Hilton, D.R., Lloyd, K.G., 2019. Forearc carbon sink reduces long-term volatile recycling into the mantle. Nature 568, 487–492. https://doi.org/10.1038/s41586-019-1131-5.

Bezard, R., Turner, S., Davidson, J.P., Macpherson, C.G., Lindsay, J.M., 2015. Seeing through the effects of crustal assimilation to assess the source composition beneath the southern Lesser Antilles Arc. J. Petrol. 56, 815–844. https://doi.org/10.1093/petrology/egv018.

Blundy, J., Cashman, K.V., Rust, A., Witham, F., 2010. A case for CO_2-rich arc magmas. Earth Planet. Sci. Lett. 290, 289–301. https://doi.org/10.1016/j.epsl.2009.12.013.

Burton, M.R., Sawyer, G.M., Granieri, D., 2013. Deep carbon emissions from volcanoes. Rev. Mineral. Geochem. 75, 323–354. https://doi.org/10.2138/rmg.2013.75.11.

Carter, L.B., Dasgupta, R., 2015. Hydrous basalt–limestone interaction at crustal conditions: implications for generation of ultracalcic melts and outflux of CO_2 at volcanic arcs. Earth Planet. Sci. Lett. 427, 202–214. https://doi.org/10.1016/j.epsl.2015.06.053.

Cernobori, L., Hirn, A., McBride, J.H., Nicolich, R., Petronio, L., Romanelli, M., 1996. Crustal image of the Ionian basin and its Calabrian margins. Tectonophysics 264, 175–189. https://doi.org/10.1016/S0040-1951(96)00125-4.

Chen, C., Förster, M.W., Foley, S.F., Liu, Y., 2021. Massive carbon storage in convergent margins initiated by subduction of limestone. Nat. Commun. 12, 1–9. https://doi.org/10.1038/s41467-021-24750-0.

Clift, P.D., 2017. A revised budget for Cenozoic sedimentary carbon subduction. Rev. Geophys. 55, 97–125. https://doi.org/10.1002/2016RG000531.

Coggon, R., Holland, T.J.B., 2002. Mixing properties of phengitic micas and revised garnet-phengite thermobarometers. J. Metamorph. Geol. 20, 683–696. https://doi.org/10.1046/j.1525-1314.2002.00395.x.

Connolly, J.A.D., 2005. Computation of phase equilibria by linear programming: a tool for geodynamic modeling and its application to subduction zone decarbonation. Earth Planet. Sci. Lett. 236, 524–541. https://doi.org/10.1016/j.epsl.2005.04.033.

Connolly, J.A.D., 2009. The geodynamic equation of state: what and how. Geochem. Geophys. Geosyst. 10, Q10014. https://doi.org/10.1029/2009GC002540.

Cook-Kollars, J., Bebout, G.E., Collins, N.C., Angiboust, S., Agard, P., 2014. Subduction zone metamorphic pathway for deep carbon cycling: I. Evidence from HP/UHP metasedimentary rocks, Italian Alps. Chem. Geol. 386, 31–48. https://doi.org/10.1016/j.chemgeo.2014.07.013.

Dale, J., Powell, R., White, R., Elmer, F., Holland, T., 2005. A thermodynamic model for Ca–Na clinoamphiboles in Na_2O–CaO–FeO–MgO–Al_2O_3–SiO_2–H_2O–O for petrological calculations. J. Metamorph. Geol. 23, 771–791. https://doi.org/10.1111/j.1525-1314.2005.00609.x.

Dasgupta, R., 2013. Ingassing, storage, and outgassing of terrestrial carbon through geologic time. Rev. Mineral. Geochem. 75, 183–229. https://doi.org/10.2138/rmg.2013.75.7.

Dasgupta, R., Hirschmann, M.M., 2010. The deep carbon cycle and melting in Earth's interior. Earth Planet. Sci. Lett. 298, 1–13. https://doi.org/10.1016/j.epsl.2010.06.039.

Davidson, J.P., 1987. Crustal contamination versus subduction zone enrichment: examples from the Lesser Antilles and implications for mantle source compositions of island arc volcanic rocks. Geochim. Cosmochim. Acta 51, 2185–2198. https://doi.org/10.1016/0016-7037(87)90268-7.

Debret, B., Sverjensky, D.A., 2017. Highly oxidising fluids generated during serpentinite breakdown in subduction zones. Sci. Rep. 7, 10351. https://doi.org/10.1038/s41598-017-09626-y.

Deegan, F.M., Troll, V.R., Freda, C., Misiti, V., Chadwick, J.P., McLeod, C.L., Davidson, J.P., 2010. Magma–carbonate interaction processes and associated CO_2 release at Merapi Volcano, Indonesia: insights from experimental petrology. J. Petrol. 51, 1027–1051. https://doi.org/10.1093/petrology/egq010.

Dutkiewicz, A., Müller, R.D., Cannon, J., Vaughan, S., Zahirovic, S., 2019. Sequestration and subduction of deep-sea carbonate in the global ocean since the Early Cretaceous. Geology 47, 91–94. https://doi.org/10.1130/G45424.1.

Epstein, G.S., Bebout, G.E., Christenson, B.W., Sumino, H., Wada, I., Werner, C., Hilton, D.R., 2021. Cycling of CO_2 and N_2 along the Hikurangi subduction margin, New Zealand: an integrated geological, theoretical, and isotopic approach. Geochem. Geophys. Geosyst. 22, e2021GC009650. https://doi.org/10.1029/2021GC009650.

Farsang, S., Louvel, M., Zhao, C., Mezouar, M., Rosa, A.D., Widmer, R.N., Feng, X., Liu, J., Redfern, S.A., 2021. Deep carbon cycle constrained by carbonate solubility. Nat. Commun. 12, 1–9. https://doi.org/10.1038/s41467-021-24533-7.

Fischer, T.P., Giggenbach, W.F., Sano, Y., Williams, S.N., 1998. Fluxes and sources of volatiles discharged from Kudryavy, a subduction zone volcano, Kurile Islands. Earth Planet. Sci. Lett. 160, 81–96. https://doi.org/10.1016/S0012-821X(98)00086-7.

Fischer, T.P., Arellano, S., Carn, S., Aiuppa, A., Galle, B., Allard, P., Lopez, T., Shinohara, H., Kelly, P., Werner, C., Cardellini, C., 2019. The emissions of CO_2 and other volatiles from the world's subaerial volcanoes. Sci. Rep. 9, 1–11. https://doi.org/10.1038/s41598-019-54682-1.

Frezzotti, M.L., Selverstone, J., Sharp, Z.D., Compagnoni, R., 2011. Carbonate dissolution during subduction revealed by diamond-bearing rocks from the Alps. Nat. Geosci. 4, 703–706. https://doi.org/10.1038/ngeo1246.

Friedlingstein, P., Houghton, R.A., Marland, G., Hackler, J., Boden, T.A., Conway, T.J., Canadell, J.G., Raupach, M.R., Ciais, P., Le Quéré, C., 2010. Update on CO_2 emissions. Nat. Geosci. 3, 811–812.

Galvez, M.E., Beyssac, O., Martinez, I., Benzerara, K., Chaduteau, C., Malvoisin, B., Malavieille, J., 2013. Graphite formation by carbonate reduction during subduction. Nat. Geosci. 6, 473–477. https://doi.org/10.1038/ngeo1827.

Galvez, M.E., Connolly, J.A., Manning, C.E., 2016. Implications for metal and volatile cycles from the pH of subduction zone fluids. Nature 539, 420–424. https://doi.org/10.1038/nature20103.

Gorce, J.S., Caddick, M.J., Bodnar, R.J., 2019. Thermodynamic constraints on carbonate stability and carbon volatility during subduction. Earth Planet. Sci. Lett. 519, 213–222. https://doi.org/10.1016/j.epsl.2019.04.047.

Gorman, P.J., Kerrick, D.M., Connolly, J.A.D., 2006. Modeling open system metamorphic decarbonation of subducting slabs. Geochem. Geophys. Geosyst. 7, Q04007. https://doi.org/10.1029/2005GC001125.

Halldorsson, S.A., Hilton, D.R., Troll, V.R., Fischer, T.P., 2013. Resolving volatile sources along the western Sunda arc. Indones. Chem. Geol. 339, 263–282. https://doi.org/10.1016/j.chemgeo.2012.09.042.

Hickey-Vargas, R., Sun, M., López-Escobar, L., Moreno-Roa, H., Reagan, M.K., Morris, J.D., Ryan, J.G., 2002. Multiple subduction components in the mantle wedge: evidence from eruptive centers in the Central Southern volcanic zone. Chile Geol. 30, 199–202. https://doi.org/10.1130/0091-7613(2002)030<0199:MSCITM>2.0.C;2.

Hilton, D.R., Fischer, T.P., Marty, B., 2002. Noble gases and volatile recycling at subduction zones. Rev. Mineral. Geochem. 47, 319–370. https://doi.org/10.2138/rmg.2002.47.9.

Holland, T., Powell, R., 1996. Thermodynamics of order-disorder in minerals: II. Symmetric formalism applied to solid solutions. Am. Mineral. 81, 1425–1437. https://doi.org/10.2138/am-1996-11-1215.

Holland, T., Powell, R., 2003. Activity–composition relations for phases in petrological calculations: an asymmetric multicomponent formulation. Contrib. Mineral. Petrol. 145, 492–501. https://doi.org/10.1007/s00410-003-0464-z.

Holland, T., Baker, J., Powell, R., 1998. Mixing properties and activity-composition and relationships of chlorites in the system MgO-FeO-Al_2O_3-SiO_2-H_2O. Eur. J. Mineral. 10, 395–406. https://doi.org/10.1127/ejm/10/3/0395.

Holland, T.J.B., Powell, R., 1998. An internally consistent thermodynamic data set for phases of petrological interest. J. Metamorph. Geol. 16, 309–343. https://doi.org/10.1111/j.1525-1314.1998.00140.x.

Holland, T.J.B., Powell, R., 2011. An improved and extended internally consistent thermodynamic dataset for phases of petrological interest, involving a new equation of state for solids. J. Metamorph. Geol. 29, 333–383. https://doi.org/10.1111/j.1525-1314.2010.00923.x.

House, B.M., Bebout, G.E., Hilton, D.R., 2019. Carbon cycling at the Sunda margin, Indonesia: a regional study with global implications. Geology 47, 483–486. https://doi.org/10.1130/G45830.1.

Johnston, F.K., Turchyn, A.V., Edmonds, M., 2011. Decarbonation efficiency in subduction zones: implications for warm Cretaceous climates. Earth Planet. Sci. Lett. 303, 143–152. https://doi.org/10.1016/j.epsl.2010.12.049.

Kelemen, P.B., Manning, C.E., 2015. Reevaluating carbon fluxes in subduction zones, what goes down, mostly comes up. Proc. Natl. Acad. Sci. USA 112, E3997–E4006. https://doi.org/10.1073/pnas.1507889112.

Kelemen, P.B., Matter, J., Streit, E.E., Rudge, J.F., Curry, W.B., Blusztajn, J., 2011. Rates and mechanisms of mineral carbonation in peridotite: natural processes and recipes for enhanced, in situ CO_2 capture and storage. Annu. Rev. Earth Planet. Sci. 39, 545–576. https://doi.org/10.1146/annurev-earth-092010-152509.

Kerrick, D.M., Connolly, J.A.D., 2001a. Metamorphic devolatilization of subducted marine sediments and the transport of volatiles into the Earth's mantle. Nature 411, 293–296. https://doi.org/10.1038/35077056.

Kerrick, D.M., Connolly, J.A.D., 2001b. Metamorphic devolatilization of subducted oceanic metabasalts: implications for seismicity, arc magmatism and volatile recycling. Earth Planet. Sci. Lett. 189, 19–29. https://doi.org/10.1016/S0012-821X(01)00347-8.

Li, K., Li, L., Pearson, D.G., Stachel, T., 2019. Diamond isotope compositions indicate altered igneous oceanic crust dominates deep carbon recycling. Earth Planet. Sci. Lett. 516, 190–201. https://doi.org/10.1016/j.epsl.2019.03.041.

Li, K., Li, L., Aubaud, C., Muehlenbachs, K., 2020. Efficient carbon recycling at the Central-Northern Lesser Antilles Arc: implications to deep carbon recycling in global subduction zones. Geophys. Res. Lett. 47, e2020GL086950. https://doi.org/10.1029/2020GL086950.

Lopez, T., Tassi, F., Aiuppa, A., Galle, B., Rizzo, A.L., Fiebig, J., Capecchiacci, F., Giudice, G., Caliro, S., Tamburello, G., 2017. Geochemical constraints on volatile sources and subsurface conditions at Mount Martin, Mount Mageik, and Trident Volcanoes, Katmai Volcanic Cluster. Alsk. J. Volcanol. Geotherm. Res. 347, 64–81. https://doi.org/10.1016/j.jvolgeores.2017.09.001.

Macpherson, C.G., Hilton, D.R., Hammerschmidt, K., 2010. No slab-derived CO_2 in Mariana Trough back-arc basalts: Implications for carbon subduction and for temporary storage of CO_2 beneath slow spreading ridges. Geochem. Geophys. Geosyst. 11, Q11007. https://doi.org/10.1029/2010GC003293.

Mann, U., Schmidt, M.W., 2015. Melting of pelitic sediments at subarc depths: 1. Flux vs. fluid-absent melting and a parameterization of melt productivity. Chem. Geol. 404, 150–167. https://doi.org/10.1016/j.chemgeo.2015.02.032.

Marschall, H.R., Schumacher, J.C., 2012. Arc magmas sourced from mélange diapirs in subduction zones. Nat. Geosci. 5, 862–867. https://doi.org/10.1038/ngeo1634.

Martin, L.A., Hermann, J., 2018. Experimental phase relations in altered oceanic crust: implications for carbon recycling at subduction zones. J. Petrol. 59, 299–320. https://doi.org/10.1093/petrology/egy031.

Marty, B., Tolstikhin, I.N., 1998. CO_2 fluxes from mid-ocean ridges, arcs and plumes. Chem. Geol. 145, 233–248. https://doi.org/10.1016/S0009-2541(97)00145-9.

Mason, E., Edmonds, M., Turchyn, A.V., 2017. Remobilization of crustal carbon may dominate volcanic arc emissions. Science 357, 290–294. https://doi.org/10.1126/science.aan5049.

Merdith, A.S., Atkins, S.E., Tetley, M.G., 2019. Tectonic controls on carbon and serpentinite storage in subducted upper oceanic lithosphere for the past 320 Ma. Front. Earth Sci. 7, 332. https://doi.org/10.3389/feart.2019.00332.

Piana Agostinetti, N., Steckler, M.S., Lucente, F.P., 2009. Imaging the subducted slab under the Calabrian Arc, Italy, from receiver function analysis. Lithosphere 1, 131–138. https://doi.org/10.1130/L49.1.

Piccoli, F., Brovarone, A.V., Beyssac, O., Martinez, I., Ague, J.J., Chaduteau, C., 2016. Carbonation by fluid-rock interactions at high-pressure conditions: implications for carbon cycling in subduction zones. Earth Planet. Sci. Lett. 445, 146–159. https://doi.org/10.1016/j.epsl.2016.03.045.

Pitzer, K., Sterner, S., 1994. Equations of state valid continuously from zero to extreme pressures for H_2O and CO_2. J. Chem. Phys. 101, 3111–3116. https://doi.org/10.1063/1.467624.

Plank, T., 2014. The chemical composition of subducting sediments. In: Keeling, Ralph F. (Ed.), Treatise on Geochemistry, vol. 4. Elsevier, Amsterdam, pp. 607–629.

Plank, T., Langmuir, C.H., 1998. The chemical composition of subducting sediment and its consequences for the crust and mantle. Chem. Geol. 145, 325–394. https://doi.org/10.1016/S0009-2541(97)00150-2.

Plank, T., Manning, C.E., 2019. Subducting carbon. Nature 574, 343–352. https://doi.org/10.1038/s41586-019-1643-z.

Plümper, O., John, T., Podladchikov, Y.Y., Vrijmoed, J.C., Scambelluri, M., 2017. Fluid escape from subduction zones controlled by channel-forming reactive porosity. Nat. Geosci. 10, 150–156. https://doi.org/10.1038/ngeo2865.

Poli, S., 2015. Carbon mobilized at shallow depths in subduction zones by carbonatitic liquids. Nat. Geosci. 8, 633–636. https://doi.org/10.1038/ngeo2464.

Poli, S., Franzolin, E., Fumagalli, P., Crottini, A., 2009. The transport of carbon and hydrogen in subducted oceanic crust: an experimental study to 5 GPa. Earth Planet. Sci. Lett. 278, 350–360. https://doi.org/10.1016/j.epsl.2008.12.022.

Polonia, A., Torelli, L., Mussoni, P., Gasperini, L., Artoni, A., Klaeschen, D., 2011. The Calabrian Arc subduction complex in the Ionian Sea: regional architecture, active deformation, and seismic hazard. Tectonics 30, TC5018. https://doi.org/10.1029/2010TC002821.

Poorter, R.P.E., Varekamp, J.C., Poreda, R.J., van Bergen, M.J., Kreulen, R., 1991. Chemical and isotopic compositions of volcanic gases from the east Sunda and Banda arcs. Indones. Geochim. Cosmochim. Acta 55, 3795–3807. https://doi.org/10.1016/0016-7037(91)90075-G.

Sano, Y., Marty, B., 1995. Origin of carbon in fumarolic gas from island arcs. Chem. Geol. 119, 265–274. https://doi.org/10.1016/0009-2541(94)00097-R.

Sano, Y., Williams, S.N., 1996. Fluxes of mantle and subducted carbon along convergent plate boundaries. Geophys. Res. Lett. 23, 2749–2752. https://doi.org/10.1029/96GL02260.

Schaaf, P., Stimac, J.I.M., Siebe, C., Macías, J.L., 2005. Geochemical evidence for mantle origin and crustal processes in volcanic rocks from Popocatépetl and surrounding monogenetic volcanoes, central Mexico. J. Petrol. 46, 1243–1282. https://doi.org/10.1093/petrology/egi015.

Schmidt, M.W., Poli, S., 1998. Experimentally based water budgets for dehydrating slabs and consequences for arc magma generation. Earth Planet. Sci. Lett. 163, 361–379. https://doi.org/10.1016/S0012-821X(98)00142-3.

Shaw, A.M., Hilton, D.R., Fischer, T.P., Walker, J.A., Alvarado, G.E., 2003. Contrasting He–C relationships in Nicaragua and Costa Rica: insights into C cycling through subduction zones. Earth Planet. Sci. Lett. 214, 499–513. https://doi.org/10.1016/S0012-821X(03)00401-1.

Sieber, M.J., Hermann, J., Yaxley, G.M., 2018. An experimental investigation of C–O–H fluid-driven carbonation of serpentinites under forearc conditions. Earth Planet. Sci. Lett. 496, 178–188. https://doi.org/10.1016/j.epsl.2018.05.027.

Staudigel, H., Hart, S.R., Schmincke, H.U., Smith, B.M., 1989. Cretaceous ocean crust at DSDP Sites 417 and 418: carbon uptake from weathering versus loss by magmatic outgassing. Geochim. Cosmochim. Acta 53, 3091–3094. https://doi.org/10.1016/0016-7037(89)90189-0.

Stewart, E.M., Ague, J.J., 2020. Pervasive subduction zone devolatilization recycles CO_2 into the forearc. Nat. Commun. 11, 1–8. https://doi.org/10.1038/s41467-020-19993-2.

Syracuse, E.M., van Keken, P.E., Abers, G.A., 2010. The global range of subduction zone thermal models. Phys. Earth Planet. Inter. 183, 73–90. https://doi.org/10.1016/j.pepi.2010.02.004.

Tajcmanová, L., Connolly, J.A.D., Cesare, B., 2009. A thermodynamic model for titanium and ferric iron solution in biotite. J. Metamorph. Geol. 27, 153–165. https://doi.org/10.1111/j.1525-1314.2009.00812.x.

Thomsen, T.B., Schmidt, M.W., 2008. Melting of carbonated pelites at 2.5–5.0 GPa, silicate–carbonatite liquid immiscibility, and potassium–carbon metasomatism of the mantle. Earth Planet. Sci. Lett. 267, 17–31. https://doi.org/10.1016/j.epsl.2007.11.027.

Thomson, A.R., Walter, M.J., Kohn, S.C., Brooker, R.A., 2016. Slab melting as a barrier to deep carbon subduction. Nature 529, 76–79. https://doi.org/10.1038/nature16174.

Tian, M., Katz, R.F., Rees Jones, D.W., 2019a. Devolatilization of subducting slabs, part I: thermodynamic parameterization and open system effects. Geochem. Geophys. Geosyst. 20, 5667–5690. https://doi.org/10.1029/2019GC008488.

Tian, M., Katz, R.F., Rees Jones, D.W., May, D.A., 2019b. Devolatilization of subducting slabs, part II: volatile fluxes and storage. Geochem. Geophys. Geosyst. 20, 6199–6222. https://doi.org/10.1029/2019GC008489.

Tonarini, S., Armienti, P., D'Orazio, M., Innocenti, F., 2001. Subduction-like fluids in the genesis of Mt. Etna magmas: evidence from boron isotopes and fluid mobile elements. Earth Planet. Sci. Lett. 192, 471–483. https://doi.org/10.1016/S0012-821X(01)00487-3.

Troll, V.R., Hilton, D.R., Jolis, E.M., Chadwick, J.P., Blythe, L.S., Deegan, F.M., Schwarzkopf, L.M., Zimmer, M., 2012. Crustal CO_2 liberation during the 2006 eruption and earthquake events at Merapi volcano. Indones. Geophys. Res. Lett. 39, L11302. https://doi.org/10.1029/2012GL051307.

Ulmer, P., Trommsdorff, V., 1995. Serpentine stability to mantle depths and subduction-related magmatism. Science 268, 858–861. https://doi.org/10.1126/science.268.5212.858.

van Keken, P.E., Hacker, B.R., Syracuse, E.M., Abers, G.A., 2011. Subduction factory: 4. Depth-dependent flux of H_2O from subducting slabs worldwide. J. Geophys. Res. 116, B01401. https://doi.org/10.1029/2010JB007922.

van Keken, P.E., Wada, I., Abers, G.A., Hacker, B.R., Wang, K., 2018. Mafic high-pressure rocks are preferentially exhumed from warm subduction settings. Geochem. Geophys. Geosyst. 19, 2934–2961. https://doi.org/10.1029/2018GC007624.

van Keken, P.E., Wada, I., Sime, N., Abers, G.A., 2019. Thermal structure of the forearc subduction zones: a comparison of methodologies. Geochem. Geophys. Geosyst. 20, 3268–3288. https://doi.org/10.1029/2019GC008334.

Varekamp, J.C., Kreulen, R., Poorter, R.P.E., van Bergen, M.J., 1992. Carbon sources in arc volcanism, with implications for the carbon cycle. Terra Nova 4, 363–373. https://doi.org/10.1111/j.1365-3121.1992.tb00825.x.

Waldbaum, D.R., Thompson, J.B., 1968. Mixing properties of sanidine crystalline solutions: II. Calculations based on volume data. Am. Mineral. 53, 2000–2017.

Wallace, P.J., 2005. Volatiles in subduction zone magmas: concentrations and fluxes based on melt inclusion and volcanic gas data. J. Volcanol. Geotherm. Res. 140, 217–240. https://doi.org/10.1016/j.jvolgeores.2004.07.023.

Werner, C., Fischer, T.P., Aiuppa, A., Edmonds, M., Cardellini, C., Carn, S., Chiodini, G., Cottrell, E., Burton, M., Shinohara, H., Allard, P., 2019. Carbon dioxide emissions from subaerial volcanic regions: two decades in review. In: Orcutt, B.N., Daniel, I., Dasgupta, R. (Eds.), Deep Carbon Past to Present. Cambridge University Press, pp. 188–236.

Wilson, C.R., Spiegelman, M., van Keken, P.E., Hacker, B.R., 2014. Fluid flow in subduction zones: the role of solid rheology and compaction pressure. Earth Planet. Sci. Lett. 401, 26–274. https://doi.org/10.1016/j.epsl.2014.05.052.

Wong, K., Mason, E., Brune, S., East, M., Edmonds, M., Zahirovic, S., 2019. Deep carbon cycling over the past 200 million years: a review of fluxes in different tectonic settings. Front. Earth Sci. 7, 263. https://doi.org/10.3389/feart.2019.00263.